Aloisines, a New Family of CDK/GSK-3 Inhibitors. SAR Study, Crystal Structure in Complex with CDK2, Enzyme Selectivity, and Cellular Effects

Yvette Mettey,[†] Marie Gompel,[‡] Virginie Thomas,[‡] Matthieu Garnier,[‡] Maryse Leost,[‡] Irène Ceballos-Picot,[§] Martin Noble,[⊥] Jane Endicott,[⊥] Jean-michel Vierfond,[†] and Laurent Meijer*,[‡]

Faculté de Médecine et de Pharmacie, 34 rue du Jardin des Plantes, B.P. 199, 86005 Poitiers Cedex, France, Cell Cycle Group, Station Biologique, C.N.R.S., B.P. 74, 29682 Roscoff Cedex, Bretagne, France, INSERM U 383, Génétique, Chromosomes et Cancer, Hôpital Necker, 75015 Paris, France, and Laboratory of Molecular Biophysics, Department of Biochemistry, University of Oxford, South Parks Road, Oxford OX1 3QU, United Kingdom

Cyclin-dependent kinases (CDKs) regulate the cell cycle, apoptosis, neuronal functions, transcription, and exocytosis. The observation of CDK deregulations in various pathological situations suggests that CDK inhibitors may have a therapeutic value. In this article, we report on the identification of 6-phenyl[5*H*]pyrrolo[2,3-*b*]pyrazines (aloisines) as a novel potent CDK inhibitory scaffold. A selectivity study performed on 26 kinases shows that aloisine A is highly selective for CDK1/cyclin B, CDK2/cyclin A−E, CDK5/p25, and GSK-3α/β; the two latter enzymes have been implicated in Alzheimer's disease. Kinetic studies, as well as the resolution of a CDK2−aloisine cocrystal structure, demonstrate that aloisines act by competitive inhibition of ATP binding to the catalytic subunit of the kinase. As observed with all inhibitors reported so far, aloisine interacts with the ATP-binding pocket through two hydrogen bonds with backbone nitrogen and oxygen atoms of Leu 83. Aloisine inhibits cell proliferation by arresting cells in both G1 and G2.

Introduction

Protein kinases catalyze the phosphorylation of serine, threonine, and tyrosine residues of proteins, using adenosine triphosphate (ATP) or guanosine 5′-triphosphate (GTP) as the phosphate donor. Protein phosphorylation is considered one of the main post-translational mechanisms used by cells to finely tune their metabolic and regulatory pathways. Protein kinases (800+ in the human genome) and their counterparts, protein phosphatases, appear to be involved in most human diseases. This is the reason screening for potent and selective inhibitors of protein kinases has intensified over the past few years (reviewed in refs 1−4). In our laboratory, we have focused our efforts on two families of kinases: cyclin-dependent kinases (CDKs) and glycogen synthase kinase-3 (GSK-3). CDKs are involved in controlling the cell cycle, apoptosis, neuronal functions and neurodegeneration, transcription, and exocytosis (reviewed in refs 5−11). GSK-3, an essential element of the WNT signaling pathway, is involved in multiple physiological processes including cell cycle regulation, in which it controls the levels of cyclin D1 and β-catenin, dorsoventral patterning during development, insulin action on glycogen synthesis, axonal outgrowth, HIV-1 Tat-mediated neurotoxicity, and phosphorylation of tau, a characteristic of Alzheimer's disease (reviewed in refs 12−17). Potential applications of CDK/GSK-3 inhibitors are being evaluated against cancers, neurodegenerative disorders such as Alzheimer's disease, proliferation of protozoan parasites, and viral infections (HIV, cytomegalovirus, and herpes virus) (reviewed in ref 18).

* To whom correspondence should be addressed. E-mail: meijer@sb-roscoff.fr. Tel.: 33 (0)2.98.29.23.39. Fax: 33 (0)2.98.29.23.42.
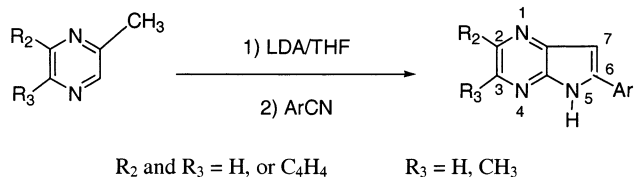† Faculté de Médecine et de Pharmacie.
‡ C.N.R.S.
§ Hôpital Necker.
⊥ University of Oxford.

Scheme 1

R₂ and R₃ = H, or C₄H₄   R₃ = H, CH₃

CDK inhibitors include the purines olomoucine,[19] roscovitine,[20,21] purvalanols,[22,23] CVT-313,[24] C2-alkylynated purines,[25] H717,[26] and NU2058,[27] piperidine-substituted purines,[28] toyocamycin,[29] flavopiridol,[30] indirubins,[31,32] paullones,[33−35] γ-butyrolactone,[36] hymenialdisine,[37] indenopyrazoles,[38] the pyrimidines NU6027[27] and CGP60474,[39] pyridopyrimidine,[40] the aminopyrimidine PNU 112455A,[41] oxindoles,[42−44] PD0183812,[45] cinnamaldehydes,[46] quinazolines,[47,48] fasclaplysin,[49] SU9516,[50] benzocarbazoles,[51] and aminothiazole[52] (reviewed in refs 18, 53−59). GSK-3 inhibitors include indirubins,[35] paullones,[35] maleimides,[60,61] and lithium.[62]

In this paper, we report on the identification of aloisines, a new family of kinase inhibitors selective for CDK1/2/5 and GSK-3α/β. These 6-phenyl[5*H*]pyrrolo-[2,3-*b*]pyrazines act in the submicromolar range by competing with ATP for binding to the kinase active site, as revealed by a CDK2−aloisine crystal structure which is presented here. Aloisine binds to the kinase ATP-binding pocket by two hydrogen bonds to the CDK2 backbone and numerous hydrophobic interactions. A comparison with the binding of other CDK inhibitors is provided. A structure/activity relationship study has been performed with 50 aloisine analogues. Finally, we show that aloisines display antiproliferative activity.
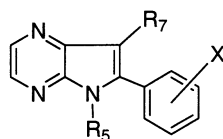
Chemistry

A series of 6-aryl[5*H*]pyrrolo[2,3-*b*]pyrazines were prepared by reaction of methylpyrazines with aromatic

Table 1. Structure, Yields, and Physical Characteristics of 6-Aryl[5*H*]pyrrolo[2,3-*b*]pyrazines
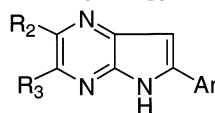
compound	R_2	R_3	Ar	yield (%)	mp (°C)	formula
1 (RP19)	H	H	2-furyl	6	232.6	$C_{10}H_7N_3O$
2 (RP6)	H	H	2-thienyl	8	260.3	$C_{10}H_7N_3S$
3 (RP128)	H	H	3-thienyl	6	230 dec	$C_{10}H_7N_3S$
4 (RP13)	H	H	2-pyridyl	8	233.1	$C_{11}H_8N_4$
5 (RP7)	H	H	phenyl	37	216.0[a]	$C_{12}H_9N_3$
6 (RP17)	H	H	1-naphthyl	17	216.4	$C_{16}H_{11}N_3$
7 (RP12)	$-C_4H_4-$		phenyl	44	260 dec[b]	$C_{16}H_{11}N_3$
8 (RP18)	H	CH_3	phenyl	26	261.8	$C_{13}H_{11}N_3$
9 (RP124)	H	H	1-(4-chlorophenyl)cyclopropyl	41	189.7	$C_{15}H_{12}N_3Cl$

[a] Lit.[64] mp 215–216 °C. [b] Lit.[64] mp 233 °C dec.

Table 2. Structure, Yields, and Physical Characteristics of Substituted 6-Phenyl[5*H*]pyrrolo[2,3-*b*]pyrazines

compound	R_5	R_7	X	yield (%)	mp (°C)	formula
10 (RP9)	H	H	2-OCH_3	27	156.9	$C_{13}H_{11}N_3O$
11 (RP109)	H	H	2-OH	22[a]	250 dec	$C_{12}H_{12}N_3O_2Br$
12 (RP10)	H	H	3-OCH_3	55	195.7	$C_{13}H_{11}N_3O$
13 (RP134)	H	H	3-OH	40[a]	258 dec	$C_{12}H_{10}N_3OBr$
14 (RP11)	H	H	4-OCH_3	48	256.1[b]	$C_{13}H_{11}N_3O$
15 (RP26)	H	H	4-OH	30[a]	255 dec	$C_{12}H_{12}N_3O_2Br$
16 (RP21)	H	H	3,5-OCH_3	50	216.7	$C_{14}H_{13}N_3O_2$
17 (RP16)	H	H	3,4,5-OCH_3	50	231.7	$C_{15}H_{15}N_3O_3$
18 (RP76)	H	H	4-F	52	244 dec	$C_{12}H_8N_3F$
19 (RP14)	H	H	4-Cl	49	250 dec[c]	$C_{12}H_8N_3Cl$
20 (RP15)	H	H	3,5-Cl	20	252 dec	$C_{12}H_7N_3Cl_2$
21 (RP77)	H	H	4-Br	24	256 dec	$C_{12}H_8N_3Br$
22 (RP8)	H	H	4-CF_3	31	238 dec	$C_{13}H_8N_3F_3$
23 (RP20)	H	H	4-CN	6	340 dec	$C_{13}H_8N_4$
24 (RP78)	H	H	4-CH_3	49	265.4	$C_{13}H_{11}N_3$
25 (RP122)	H	H	2-dioxolyl	43	265.6	$C_{15}H_{13}N_3O_2$
26 (RP129)	H	H	4-$N(CH_3)_2$	5	271 dec	$C_{14}H_{14}N_4$
27 (RP95)	H	CH_3	4-OCH_3	47	221.6	$C_{14}H_{13}N_3O$
28 (RP96)	H	CH_3	4-OH	41[a]	262 dec	$C_{13}H_{12}N_3OBr$
29 (RP123)	H	H	3,4-OCH_3	51	230.2	$C_{15}H_{15}N_3O_2$
30 (RP80)	H	CH_3	4-Cl	44	260 dec	$C_{13}H_{10}N_3Cl$
31 (RP125)	H	CH_3	$OSO_2N(CH_3)_2$	72	235.1	$C_{15}H_{16}N_4SO_3$
32 (RP127)	H	$(CH_2)_2CH_3$	OCH_3	26	188.5	$C_{16}H_{17}N_3O$
33 (RP132)	H	$(CH_2)_2CH_3$	OH	50[a]	244 dec	$C_{15}H_{16}N_3OBr$
34 (RP110)	H	$CH_2-CH=CH_2$	4-OCH_3	36	193.8	$C_{16}H_{15}N_3O$
35 (RP126)	H	$(CH_2)_2CH_2Cl$	4-OCH_3	10	178 dec	$C_{16}H_{16}N_3OCl$
36 (RP102)	H	$CH(CH_3)_2$	4-OCH_3	2	204.8	$C_{16}H_{17}N_3O$
37 (RP90)	H	$CH(CH_3)_2$	4-Cl	15	208.6	$C_{15}H_{14}N_3Cl$
38 (RP106)	H	$(CH_2)_3CH_3$	4-OCH_3	32	183.8	$C_{17}H_{19}N_3O$
39 (RP107)	H	$(CH_2)_3CH_3$	4-OH	66[a]	281.4	$C_{16}H_{17}N_3O$
40 (RP108)	H	$(CH_2)_3CH_3$	4-Cl	70	200.0	$C_{16}H_{16}N_3Cl$
41 (RP111)	H	$(CH_2)_6CH_3$	4-OCH_3	50	132.5	$C_{20}H_{25}N_3O$
42 (RP104)	H	$CH_2-C_3H_5$	4-OCH_3	30	193.9	$C_{17}H_{17}N_3O$
43 (RP112)	H	$CH_2-C_3H_5$	4-OH	54[a]	260 dec	$C_{16}H_{18}N_3O_2Br$
44 (RP92)	H	$CH_2-C_6H_5$	H	24	209.8	$C_{19}H_{15}N_3$
45 (RP91)	H	$CH_2-C_6H_5$	Cl	20	266.3	$C_{19}H_{14}N_3Cl$
46 (RP98)	H	$CH_2-C_6H_{11}$	4-OCH_3	1	220.3	$C_{20}H_{23}N_3O$
47 (RP99)	H	$CH_2-C_6H_{11}$	4-Cl	4	203.5	$C_{19}H_{20}N_3Cl$
48 (RP22)	CH_3	H	H	54	72.3	$C_{13}H_{11}N_3$

[a] Calculated from methoxy compound. [b] Lit.[64] mp 238–240 °C. [c] Lit.[64] mp 250 °C dec.

nitriles, using our previously described procedure[63] (Scheme 1). Compounds **1**–**9** were obtained in moderate or poor yields, together with 1-amino-1-aryl-2-(2-pyrazinyl)ethene. Yields and physical characteristics of the products **1**–**9** are recorded in Table 1. From biological results, we similarly prepared a series of substituted 6-phenyl[5*H*]pyrrolo[2,3-*b*]pyrazines from methyl- or alkylpyrazines and appropriate substituted benzonitriles. Alkylpyrazines were obtained by reaction of pyrazinylmethyllithium with bromoalkanes, and ben-

zonitriles were commercially available products. Demethylation of methoxy compounds was achieved by refluxing in 47% hydrobromidic acid at 126 °C. The time required for demethylation varied from 3 to 20 h. The yields were moderate. These results are presented in Table 2.

We also prepared 6-[1-(4-chlorophenyl)1-cyclopropyl]-7-methyl[5*H*]pyrrolo[2,3-*b*]pyrazine (**49**, RP 130) and 2-(4-methoxyphenyl)[1*H*]pyrrolo[2,3-*b*]pyridine[64] (**50**, RP 97) from 2-picoline and *p*-methoxybenzonitrile (Table 3).
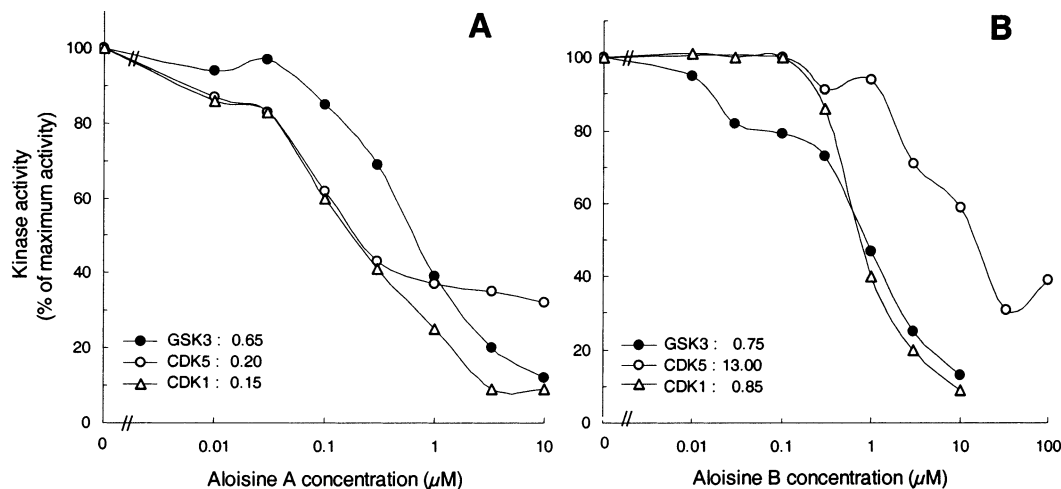
Figure 1. Aloisine A and B inhibit CDK1/cyclin B, CDK5/p25, and GSK-3β. Kinases were assayed as described in the Experimental Section in the presence of increasing concentrations of aloisines A and B. Activity is presented as percentage of maximal activity, i.e., measured in the absence of inhibitors.

Table 3.

compound	yield (%)	mp (°C)	formula
49 (RP130)	41	223.9	$C_{16}H_{14}N_3Cl$
50 (RP97)	20	206.2[a]	$C_{14}H_{12}N_2O$

[a] Lit.[64] mp 205−206 °C.

Results and Discussion

Aloisines, a Family of CDK1/2 and GSK-3 Inhibitors. Two decades ago, we proposed an original method for the one-pot synthesis of [5*H*]pyrrolo[2,3-*b*]pyrazines.[63] While screening for new protein kinase inhibitors, we discovered that some of these diazaindoles were potent inhibitors of CDKs and GSK-3β (Figure 1; Tables 4 and 5). In the presence of 15 μM ATP, the compounds were found to inhibit CDKs and GSK-3 in the submicromolar range (Figure 1). Given the key function of both CDK5 and GSK-3 in the hyperphosphorylation of tau in Alzheimer's disease, we named this family of compounds "aloisines", following the first name of Dr. Alzheimer, Alois. Aloisine represents the unsubstituted 6-phenyl[5*H*]pyrrolo[2,3-*b*]pyrazine scaffold. Two aloisines, aloisine A (**39**, RP107) and aloisine B (**37**, RP90), were selected for further studies to investigate their molecular mechanism of action, cocrystallization with CDK2, selectivity, and cellular effects (see below).
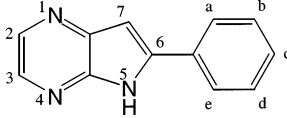
Aloisine Is a Competitive Inhibitor of ATP Binding. To investigate the mechanism of aloisine's action, kinetic experiments were performed by varying both ATP levels and aloisine A concentrations (Figure 2). These experiments were performed with CDK1/cyclin B, CDK5/p25, and GSK-3β. Double-reciprocal plotting of the data demonstrates that aloisine A acts as a competitive inhibitor for ATP. These results are in complete agreement with the localization of aloisine B within the ATP-binding pocket of CDK2 (see below).

Aloisine−CDK2 Cocrystal Structure, Overall Conformation of Protein and Ligand, and Comparison with Other CDK2−Inhibitor Structures. Aloisine B was chosen for soaking into monomeric CDK2 crystals (Table 6). Aloisine B occupies the CDK2 ATP-binding site and makes two hydrogen bonds to the CDK2 backbone within the hinge sequence that links the two lobes of the kinase (Figure 3). Unlike the natural ligand, ATP, aloisine B does not interact with the backbone oxygen of Glu81, but instead it accepts and donates a hydrogen bond respectively from the backbone nitrogen and oxygen atoms of Leu83 (Figure 4).[65,66] This hydrogen-bonding pattern has previously been observed in the structures of monomeric CDK2 in complex with olomoucine,[66] roscovitine,[21] purvalanol B,[22] OL567,[25] and H717.[26] The CDK2 ATP-binding site is tolerant of a number of positions for the planar heterocyclic ring systems which are a characteristic of the CDK inhibitors identified to date (reviewed in ref 54). The position of the aloisine B fused ring system within the CDK2 ATP-binding site most closely resembles that of indirubin-5-sulfonate[31] and oxindole-3.[43] However, being smaller than indirubin-5-sulfonate and in a different orientation to oxindole-3, aloisine B does not fill the back of the ATP-binding cleft and form an equivalent edge-to-ring stacking interaction with the side chain of Phe80 (Figure 5).

In the apo-CDK2 structure,[65] and in other monomeric CDK2−inhibitor complex structures,[21,22,27,31,37,66−68] two regions of CDK2 have been reported to be flexible. These regions have been excluded from some CDK2−inhibitor models and constitute the loop connecting strand β3 to helix αC, and the "activation segment" containing Thr160, which is phosphorylated in the fully active CDK2−cyclin A complex.[69] The CDK2−aloisine B complex also is flexible in the first of these regions. Interpretable electron density confirms that the conformation of the activation segment resembles that seen in the monomeric CDK2−ATP complex, although this electron density is rather weak (<0.15 e⁻ Å⁻³) for residues 155−162. Thus, aloisine B binding to CDK2 does not significantly decrease the temperature factors of this segment, as has been reported for certain compounds in a series of guanine-based inhibitors.[27] This might be because the aloisine B isopropyl group that binds in the ATP ribose site is much smaller than the substituents of the O6-substituted guanine series and does not contact CDK2 in this region (Figures 5A and 6A).

The aloisine B 4-chlorophenyl group points out of the ATP-binding site cleft toward the surface of the CDK2 C-terminal domain (Figure 3). A superposition of the structures of the CDK2−aloisine B and CDK2−oxin-

Table 4. Structure/Activity Relationship of Aloisines[a]

compound	a	b	c	d	7	CDK1/cyclin B	CDK5/p25	GSK-3
5 (RP7)						5.00	4.00	2.30
10 (RP9)	OCH_3					20.00	23.00	3.30
11 (RP109)	OH					2.50	3.00	6.50
12 (RP10)		OCH_3				13.00	10.00	3.20
13 (RP134)		OH				2.50		
14 (RP11)			OCH_3			2.00	4.00	1.10
15 (RP26)			OH			1.20	1.00	1.20
16 (RP21)		OCH_3		OCH_3		100.00	>100.00	60.00
17 (RP16)		OCH_3	OCH_3	OCH_3		100.00	>100.00	85.00
18 (RP76)			F			2.30	1.00	1.90
19 (RP14)			Cl			1.80		
20 (RP15)		Cl		Cl		>100.00	>100.00	>100.00
21 (RP77)			Br			4.00	>100.00	6.00
22 (RP8)			CF_3			6.00	>100.00	7.20
24 (RP78)			CH_3			3.00	10.00	2.60
23 (RP20)			CN			3.00	13.00	4.80
26 (RP129)			$N(CH_3)_2$			20.00	>100.00	12.00
27 (RP95)			OCH_3		CH_3	0.30	0.80	0.46
29 (RP123)		OCH_3	OCH_3		CH_3	1.10	1.00	2.00
32 (RP127)			OCH_3		$(CH_2)_2CH_3$	0.40	0.50	0.40
35 (RP126)			OCH_3		$(CH_2)_3Cl$	1.30	3.00	2.50
36 (RP102)			OCH_3		$CH(CH_3)_2$	1.00	2.00	0.50
34 (RP110)			OCH_3		$CH_2-CH=CH_2$	1.00	2.00	0.60
38 (RP106)			OCH_3		$(CH_2)_3CH_3$	0.70	1.50	0.92
41 (RP111)			OCH_3		$(CH_2)_6CH_3$	7.00	>100.00	>10.00
42 (RP104)			OCH_3		$CH_2C_3H_5$	1.00	>100.00	1.10
46 (RP98)			OCH_3		$CH_2C_6H_{11}$	5.00	>100.00	6.80
31 (RP125)			$O-SO_2-N(CH_3)_2$		CH_3	0.70	0.90	0.50
30 (RP80)			Cl		CH_3	0.40	5.00	1.70
37 (RP90) (aloisine B)			Cl		$CH(CH_3)_2$	0.85	13.00	0.75
40 (RP108)			Cl		$(CH_2)_3CH_3$	0.20	>100.00	5.90
45 (RP91)			Cl		$CH_2C_6H_5$	40.00	>100.00	6.80
44 (RP92)					$CH_2C_6H_5$	2.00	>100.00	1.00
47 (RP99)			Cl		$CH_2C_6H_{11}$	10.00	>100.00	8.00
28 (RP96)			OH		CH_3	0.25	0.20	0.52
33 (RP132)			OH		$(CH_2)_2CH_3$	25.00	1.20	1.80
39 (RP107) (aloisine A)			OH		$(CH_2)_3CH_3$	0.15	0.20	0.65
43 (RP112)			OH		$CH_2C_3H_5$	50.00	>100.00	3.00

[a] Enzyme activities were assayed as described in the Experimental Section, in the presence of increasing concentrations of aloisines. IC_{50}'s were calculated from the dose−response curves.

dole-3 complexes (Figure 6B) shows that the positions of the aloisine B 4-chlorophenyl and the oxindole-3 benzylsulfonamide groups are overlaid so that the aloisine B chlorine atom occupies the same position as the sulfur atom of the oxindole-3 sulfonamide group. However, the chlorine atom cannot mimic the sulfonamide interactions with the backbone nitrogen and the side chain of Asp86 through one of its oxygens and its amine group, respectively. The purvalanol B 3-chloro-4-carboxyanilino group also probes this region of CDK2.[22] In this case, the chlorine atom has a polar interaction with the side chain of Asp86, and the carboxyl group is in van der Waals contact with the side chain of Lys89. As the anilino group of purvalanol B is not constrained to be coplanar with its purine ring, it adopts a conformation rather different from that of aloisine B and oxindole-3. This conformation allows it to exploit the potential stacking interaction of its aromatic ring with the planar peptide bond between His84 and Gln85. Because it is conjugated with its heterocyclic ring system, the phenyl ring of aloisine B cannot adopt this conformation.

Aloisines: Structure/Activity Relationship. A variety of aloisine derivatives were synthesized, as well

as a few related compounds. The IC_{50} values of all compounds against CDK1/cyclin B, CDK5/p25, and GSK-3β were determined from dose−response curves and are presented in Tables 4 and 5. This modest structure/activity study constitutes only the first steps of a larger study that should be continued on the basis of the data given by the aloisine B−CDK2 cocrystal structure and its comparison with other inhibitor−CDK2 structures. Nevertheless, these preliminary data provide some key SAR features.

First, as the three nitrogen atoms of the phenylpyrrolo[2,3-*b*]pyrazine skeleton are engaged in hydrogen bonds with the Leu83 and Lys33 residues of CDK2 (see above, and Figures 4 and 5), substitutions on these three positions (i.e., 1, 4, and 5) are to be excluded. Furthermore, replacement of any of the nitrogen atoms in this skeleton by a carbon abolishes the inhibitory activity (Tables 4 and 5). Replacement of the nitrogen atom in position 1 by a carbon (**50**), or substitution of the nitrogen atom in position 5 by a methyl group (**48**), results in a dramatic decrease in the inhibitory activity.

Thus, substitutions on other positions (a−e, 7) were undertaken to orientate the synthesis of derivatives toward improved CDK and GSK-3 inhibitory activity.

Table 5. Structure/Activity Relationship of Aloisine-Related Compounds[a]
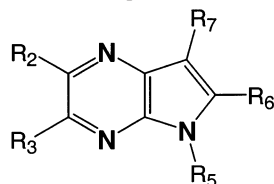
N°	R2, R3	R5	R6	R7	CDK1/ cyclin B	CDK5/ p25	GSK-3
1(RP 19)	H, H	H	(2-furyl)	H	12	9.30	15
2 (RP6)	H, H	H	(2-thienyl)	H	7.00	2.00	1.20
3 (RP128)	H, H	H	(3-thienyl)	H	2.30	1.00	0.80
4 (RP13)	H, H	H	(2-pyridyl)	H	21.00	53.00	15.00
6 (RP17)	H, H	H	(naphthyl)	H	>100.00	80.00	27.00
7 (RP12)	R2, R3 (fused benzo)	H	(phenyl)	H	>100.00	>100.00	>100.00
9 (RP124)	H, H	H	(cyclopropyl-4-chlorophenyl)	H	30.00	100.00	1.00
49 (RP130)	H, H	H	(cyclopropyl-4-chlorophenyl)	CH₃	25.00	100.00	18.00
25 (RP122)	H, H	H	(phenyl-1,3-dioxolane)	H	8.00	15.00	20.00
8 (RP18)	R2: H R3: CH₃	H	(phenyl)	H	69.00	100.00	>100.00
48 (RP22)	H, H	CH₃	(phenyl)	H	100.00	7.00	>100.00

N°	Structure	CDK1/ cyclin B	CDK5/ p25	GSK-3
50 (RP97)	(7-azaindole-2-(4-methoxyphenyl))	60.00	-	-
2-phenylindole	(2-phenylindole)	>100	-	-

[a] Enzyme activities were assayed as described in the Experimental Section, in the presence of increasing concentrations of aloisines. IC$_{50}$'s were calculated from the dose−response curves and are presented in micromolar.

We first focused on position c, without any other additional substitution. If we consider the aloisine B−CDK2 cocrystal structure and admit that the inhibitor has the same position in the ATP-binding pocket, regardless of what moiety is in position c, none of the substituents tested in this position is within a distance of 4 Å from the side-chain CO$_2$H or backbone NH of Asp86. This distance is too large to allow the formation of hydrogen bonds. It would be interesting to test larger substituents which could get close enough to these functions to provide hydrogen bonds. Indeed, from the comparison with the oxindole−CDK2 complex structure, in which the SO$_2$NH$_2$ group sits very close to that of the aloisine B chlorine, one can imagine some interesting substitutions at position a. The SO$_2$NH$_2$ moiety makes two hydrogen bonds with CDK2: one of the O atoms accepts a hydrogen bond from the backbone NH of Asp86, and the NH$_2$ group donates to the side-chain
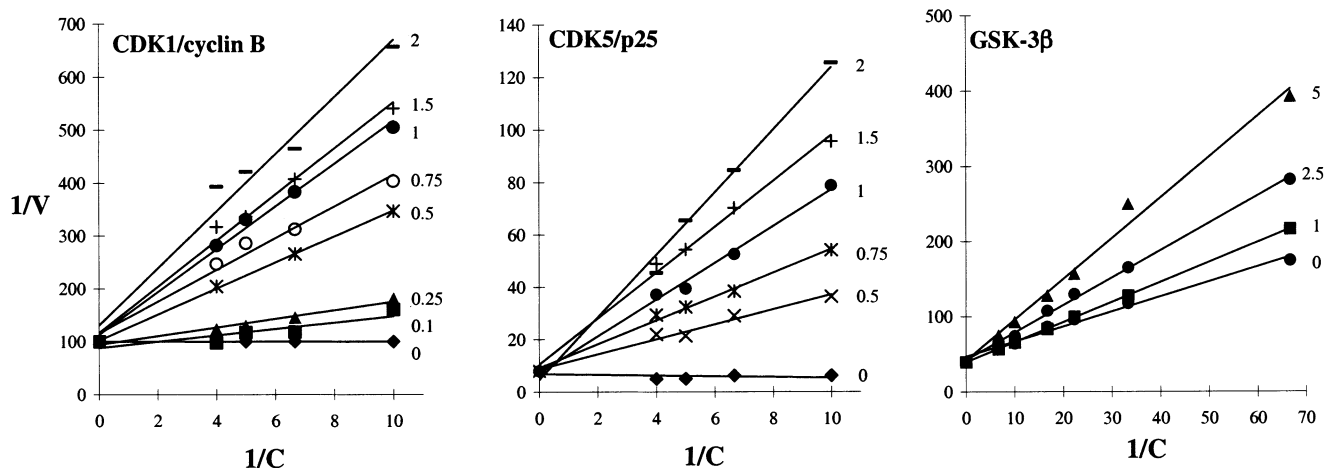
Figure 2. Aloisine A acts by competing with ATP. Double reciprocal plots of kinetic data from assays of CDK1/cyclin B (A), CDK5/p25 (B), and GSK-3β (C). Kinase activities at different concentrations of aloisine A (indicated in micromolar). Enzyme activities were assayed as described in the Experimental Section. ATP concentrations in the reaction mixture varied from 0.1 to 0.25 mM (CDK1 and CDK5) or from 0.015 to 0.15 mM (GSK-3β). The concentrations of histone H1 (A, B) and GS-1 (C) were kept constant at 0.7 mg/mL and 6.7 μM, respectively.

Table 6. CDK2−Aloisine B Cocrystal Structure: Statistics of the Dataset Used and of the Refined Structure

cell dimensions (Å)	53.0, 71.3, 71.9
maximal resolution (Å)	1.9
observations	79 169
unique reflections (completeness, %)	21 476 (97.9)
$R_{merge}{}^a$	0.081
mean $I/\sigma(I)$	7.6
highest resolution bin (Å)	2.00−1.90
completeness (%)	97.9
mean I/mean $\sigma(I)$	2.1
R_{merge}	0.36
protein atoms	2340
residues	1−36, 44−298
other atoms	188 water; 19 aloisine B
resolution range (Å)	72.55−1.90
$R_{conv}{}^b$	0.17
$R_{free}{}^c$	0.23
mean protein temperature factors (Å)^b	23.8
mean ligand temperature factors (Å)^b	34.8

^{a} $R_{merge} = [\sum_h \sum_j I_{h,j} - \bar{I}_h]/[\sum_h \sum_j I_{h,j}]$, where $I_{h,j}$ is the intensity of the jth observation of unique reflection h. ^{b} $R_{conv} = [\sum_h ||F_{oh}| - |F_{ch}||/[\sum_h |F_{oh}|]$, where F_{oh} and F_{ch} are the observed and calculated structure factor amplitudes for reflection h. ^{c} R_{free} is equivalent to R_{conv} but is calculated using a 5% disjoint set of reflections excluded from the least-squares refinement stages.

CO_2H of Asp86. Thus, groups such as $CONH_2$, CO_2H, or SO_3H, with both donating and accepting capability, might interact potently with the Asp86 residue. Among the moieties tested so far, the OH group turned out to be the best (followed by OCH_3 and Cl, respectively).

Much of the work was then dedicated to substituting position 7 with either −OH, −OCH_3, or −Cl in position c. From this study, two major facts emerged. First, the introduction of bulky groups in position 7 seems to be detrimental for the CDK and GSK-3 inhibitory activity. Second, small aliphatic saturated alkyl chains [$(CH_2)_n$, $n = 1-4$] give the best results among the groups tested.

Moreover, the aloisine-related molecules did not show good results, except for the thienyl-pyrrolo[2,3-*b*]pyrazine compounds, which approximately equaled their aloisine homologues' performances on CDK1, CDK5, and GSK-3 (Table 5).

Aloisines: Kinase Selectivity. Aloisine A, the most active aloisine so far, was tested for selectivity on 26 highly purified kinases (Table 7). Kinase activities were assayed with appropriate substrates (for example, his-
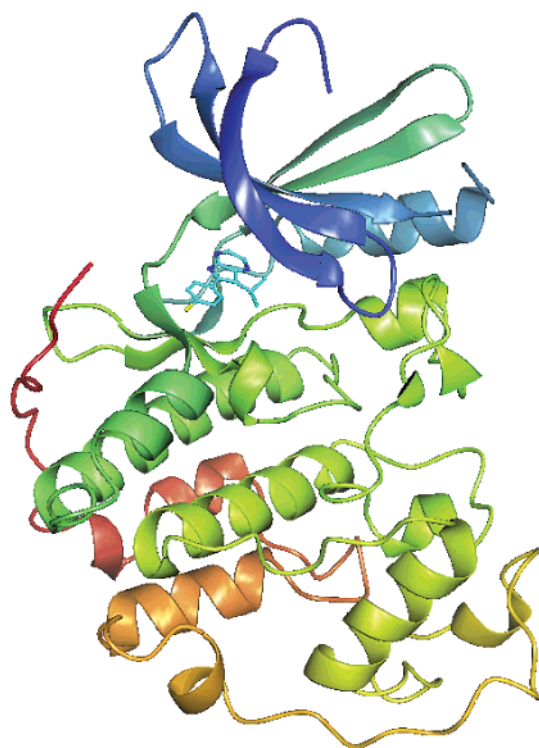

Figure 3. Binding of aloisine B to CDK2. CDK2 is drawn in ribbon representation and color-ramped from blue to red, starting at the N-terminus. The N-terminal lobe is dominated by a five-stranded antiparallel β-sheet, and the C-terminal lobe is predominantly α-helical. Aloisine B is drawn in ball-and-stick mode bound at the ATP-binding site, which lies in the cleft between the two domains. Aloisine B carbon atoms are colored cyan, nitrogen atoms blue, and the chlorine atom yellow.

tone H1, casein, myelin basic protein, and peptides), with 15 μM ATP and in the presence of increasing concentrations of aloisine A. IC_{50} values were estimated from the dose−response curves and are presented in Table 7. Most kinases tested were inhibited poorly or not at all ($IC_{50} > 10$ μM). However, two families of kinases, GSK-3α/β and CDKs, were strongly sensitive to aloisine A (IC_{50}'s of 0.65 and 0.15 μM, respectively) (Figure 1; Table 7). Among the CDKs, CDK1, CDK2,
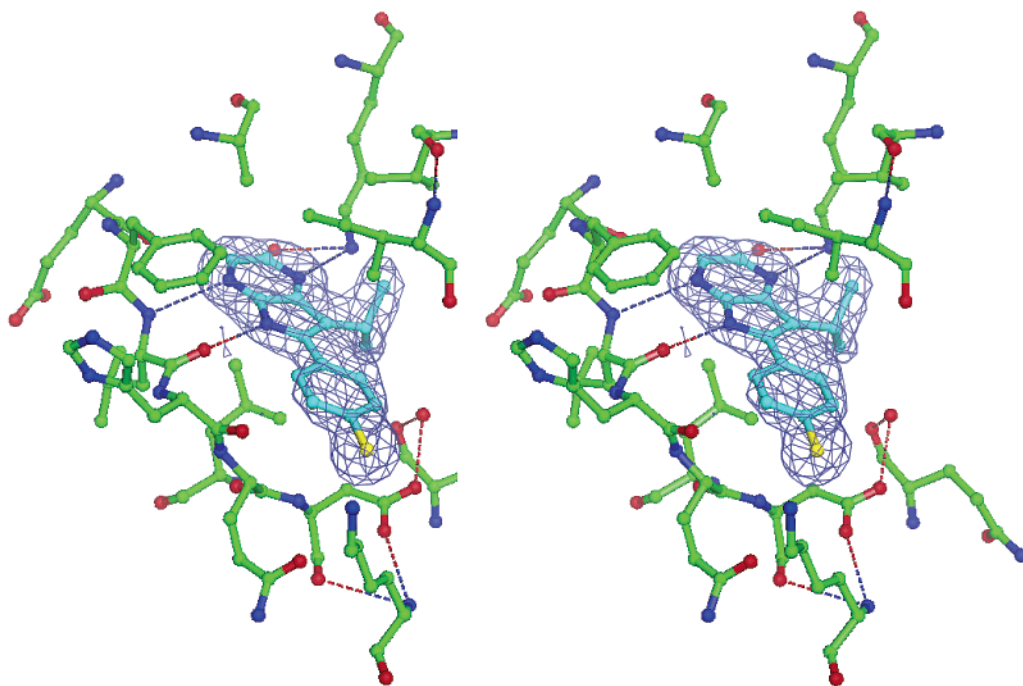
Figure 4. Stereoview showing the interactions between aloisine B and the CDK2 ATP-binding site. Residues that lie within 4 Å of the bound aloisine B molecule are drawn in ball-and-stick mode. Aloisine B carbon atoms are drawn in cyan and those of CDK2 in green. Oxygen atoms are colored red, nitrogen atoms blue, and the chlorine atom yellow. Dotted lines represent hydrogen bonds (d(O→N) or d(N−O) < 3.4 Å) between aloisine B and the backbone nitrogen and oxygen atoms of Leu83. The figure also includes $(2F_o − F_c)\alpha_{calc}$ electron density for aloisine B, calculated at the end of refinement using map coefficients output from REFMAC with resolution between 20 and 1.9 Å. The map is contoured at a level of 0.19 e$^−$ Å^{-3}, corresponding to 1.0 times the rms deviation of the map from its mean value.
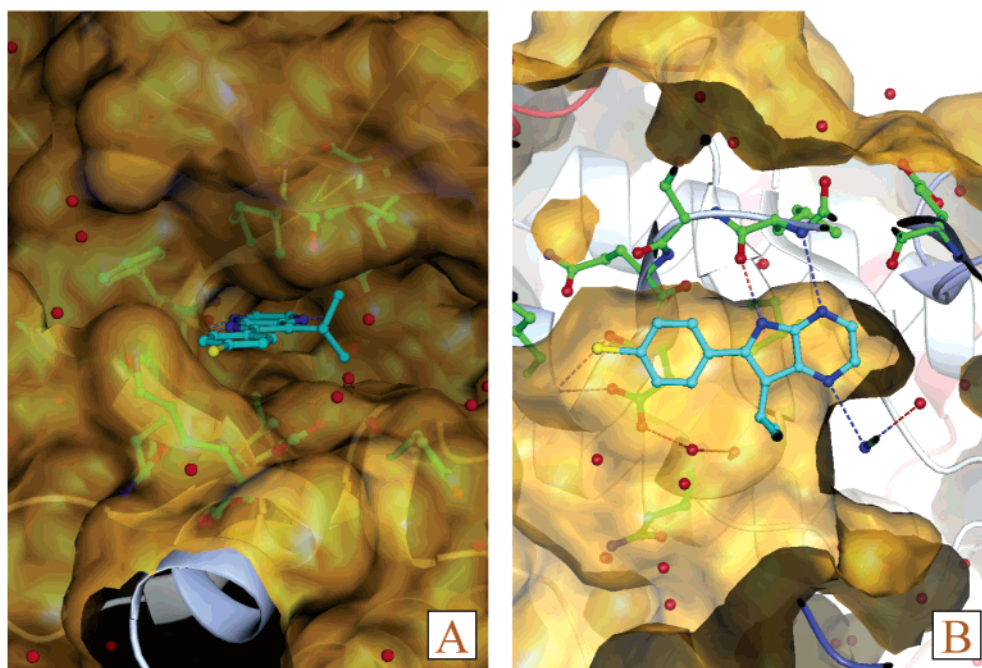
Figure 5. Molecular surface of the CDK2 ATP-binding site in the CDK2−aloisine B complex. The Connelly molecular surface was calculated within the program Aesop using a probe radius of 1.4 Å and is shown in gold. Secondary structural elements are colored blue. Atoms of the CDK2 structure seen through the surface representation are rendered in ball-and-stick mode and colored green, and carbon atoms of aloisine B are drawn in cyan. (A) View looking into the active site with the N-terminal domain above. Aloisine B binds into the adenine-binding pocket but does not contact residues in the ribose-phosphate binding site. (B) View looking down onto the surface of the CDK2 C-terminal domain in the ATP-binding pocket from the N-terminal domain. The hydrogen bonds between the backbone oxygen and nitrogen atoms of Leu83 and aloisine B are drawn as dotted lines. There is a third hydrogen bond between aloisine B and the ε-amino group of Lys33.

and CDK5, but not CDK4, were inhibited by aloisine A. This is reminiscent of other CDK inhibitors, such as purines,[22,70] hymenialdisine,[37] paullones,[33,34] and in-dirubins,[31] which inhibit CDK1/2/5 but have much less or no effect on CDK4/6. Although aloisines appear to be remarkably specific to CDKs and GSK-3, the actual
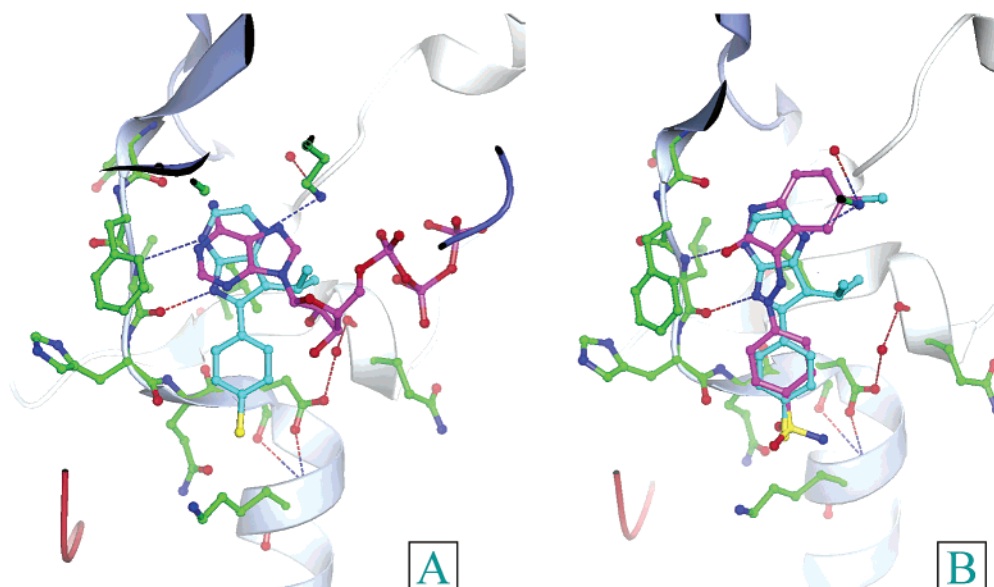
Figure 6. Superposition of aloisine B and ATP (A) and aloisine B and oxindole-3 (B) bound to CDK2. The CDK2–aloisine B complex is shown in each case with CDK2 carbon atoms in green, aloisine B carbon atoms in cyan, and ATP (A) or oxindole-3 (B) carbon atoms colored magenta, respectively. The structures were superimposed on the basis of all protein atoms. In each figure, the fold of CDK2 is rendered in ribbon mode, and the residues identified in Figure 3 are drawn in ball-and-stick representation.

Table 7. Kinase Inhibition Selectivity of Aloisine A[a]

$\leq 1\ \mu M$	$1-10\ \mu M$	$> 10\ \mu M$

Protein Kinases	IC$_{50}$ (μM)
CDK1/cyclin B	0.15
CDK2/cyclin A	0.12
CDK2/cyclin E	0.40
CDK4/cyclin D1	>100.00
CDK5/p35	0.16
erk1	18.00
erk2	22.00
c-raf	>100.00
MAPKK	>100.00
c-Jun N-terminal kinase	3.3–10
protein kinase C α	>100.00
protein kinase C β1	>100.00
protein kinase C β2	>100.00
protein kinase C γ	>100.00
protein kinase C δ	>100.00
protein kinase C ϵ	>100.00
protein kinase C η	>100.00
protein kinase C ζ	>100.00
cAMP-dependent protein kinase	100.00
cGMP-dependent protein kinase	100.00
GSK3-α	0.50
GSK3-β	1.50
Casein kinase 1	>100.00
Casein kinase 2	>100.00
Insulin receptor tyrosine kinase	60.00
PIM 1	>10.00

[a] Enzyme activities were assayed as described in the Experimental Section, in the presence of increasing concentrations of aloisine A. IC$_{50}$'s were calculated from the dose–response curves and are presented in micromolar.

spectrum of their intracellular targets remains to be identified. For this purpose, we are currently designing an immobilized aloisine matrix to purify aloisine-binding proteins by the affinity chromatography method described for purines[71] and paullones.[72]

Cellular Effects of Aloisines. The cellular effects of aloisine A were evaluated on undifferentiated human teratocarcinoma cells (NT2) and differentiated postmitotic neurons (hNT). First, NT2 cells were treated or not with 10 μM aloisine A and counted at different intervals over time. Results show that aloisine A completely blocks the proliferation of dividing cells, as the number of aloisine A-treated NT2 cells remains essentially constant, while control cells, exposed to vehicle (0.1% DMSO), double every 24 h (Figure 7A). The time course also shows that very few cells actually die in the presence of aloisine A. This lack of toxicity is further supported by the reversibility of aloisine A's effect (Figure 7B). The proliferation inhibitory activity of aloisine A was dose-dependent, with an IC$_{50}$ of 7 μM (Figure 7C). A slightly higher IC$_{50}$ value (10.5 μM) was found for hNT viability (Figure 7D).

The effect of aloisine A on the cell cycle distribution was investigated for NT2 cells by flow cytometry. Unsynchronized cells (Figure 7E) were exposed to 20 μM aloisine A for 40 h (Figure 7F). The proliferation arrest induced by aloisine A in exponentially growing cells was clearly accompanied by an accumulation of the G2/M phase. No signs of apoptosis were detectable, confirming the lack of apparent toxicity observed before.

We next investigated the effects of aloisine A on NT2 cells synchronized either in G0/G1 by serum deprivation or in G2/M by nocodazole treatment (Figure 8). Serum deprivation for 24 h led to a significant increase of cells in G0/G1 (Figure 8A). Cells were then re-exposed to a serum-enriched media for 40 h in the absence (Figure 8B) or presence (Figure 8C) of 20 μM aloisine A. Aloisine A-treated cells remained essentially in G0/G1, with a small additional accumulation of G2/M cells, most probably derived from the initial S phase subpopulation (Figure 8C). Control cells redistributed in a classical cell cycle pattern (Figure 8B). Nocodazole treatment for 24 h led to a massive accumulation of cells in G2/M (Figure 8D). Cells were then washed to remove nocodazole and incubated for 40 h in the absence (Figure 8E) or
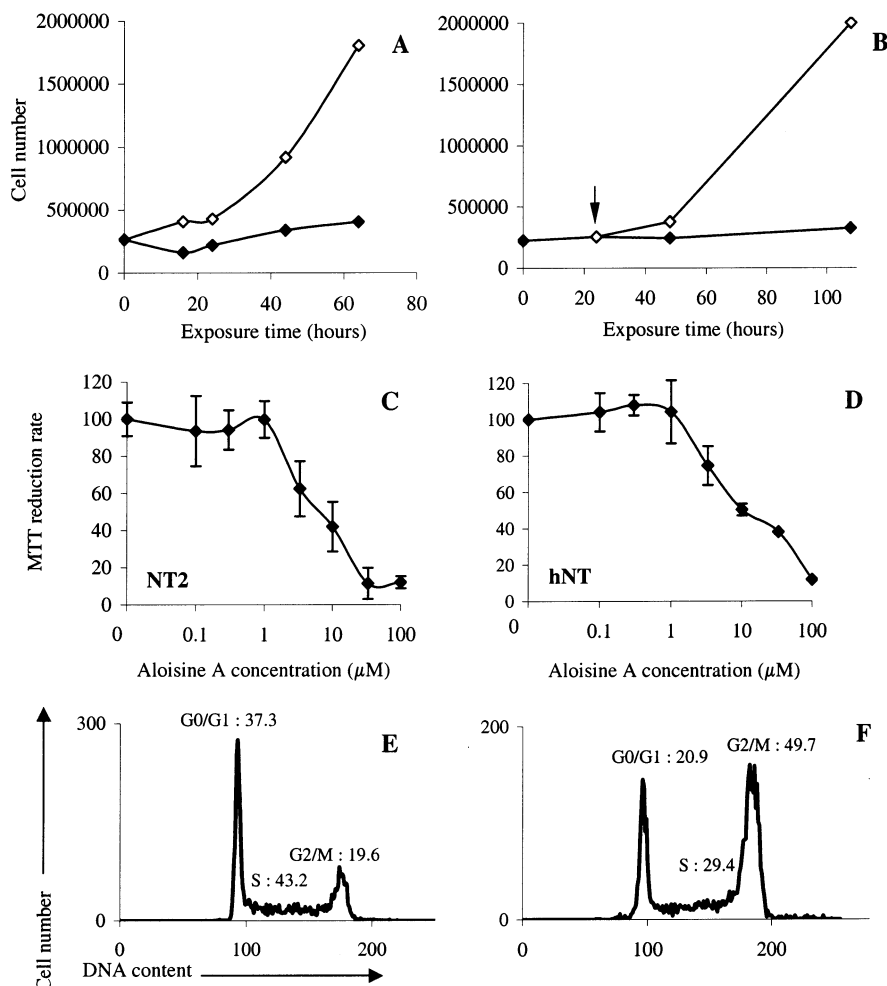
Figure 7. Reversible inhibition of exponential cell growth by aloisine A. (A) Exponentially growing NT2 cells were treated either with 10 μM aloisine A (◆) or 0.1% DMSO (◇). Cells were harvested by trypsinization at the indicated times and counted. (B) Cell growth arrest induced by aloisine A is reversible. Exponentially growing NT2 cells were treated with 10 μM aloisine A for 24 h (arrow). They were then washed with PBS and maintained in the presence of either 10 μM aloisine A (◆) or 0.1% DMSO (◇). Cells were harvested by trypsinization at the indicated times and counted. (C) Dose-dependent antiproliferative effects of aloisine A. NT2 cells were exposed to several concentrations of aloisine A for 40 h. Thereafter, cells were incubated with MTT, and the antiproliferative effect of aloisine A was evaluated through the measurement of the inhibition of cellular reduction of MTT to MTT formazan, a reflection of the density of living cells. Cell viability is expressed as percentage of the 0.1% DMSO-treated control. The values are given as the mean ± SD ($n = 8$). (D) Antiproliferative effect of aloisine A on hNT cells. On day 5 after the second replate, hNT cells were exposed to several concentrations of aloisine A for 40 h. Thereafter, cells were incubated with MTT, and the toxic effect of aloisine A was evaluated as described above ($n = 4$). (E) Cell cycle distribution of unsynchronized NT2 cells treated for 40 h with 0.1% DMSO. The same profile was observed for untreated cells. (F) Cell cycle distribution of unsynchronized NT2 cells treated for 40 h with 20 μM aloisine, leading to an accumulation of G2/M arrested cells.

presence (Figure 8F) of 20 μM aloisine A. Forty hours after nocodazole withdrawal, control cells redistributed in the various cell cycle phases (Figure 8E). In contrast, the majority of cells exposed to aloisine A after nocodazole treatment remained in G2/M (Figure 8F), precluding the increase in G1/G0 seen in control cells. A small sub-G2 peak may indicate a minor onset of apoptotic cell death.

Altogether, these data indicate that aloisine A has antiproliferative properties and that it is able to block both the exit from G0/G1 and the exit from G2/M, suggesting the existence of several intracellular targets. A G1 arrest correlates with aloisine A's high potency against CDK2/cyclin E. The inability to enter S phase might also result from inhibition of GSK-3, a kinase known to be involved in cyclin D1 degradation.[73] The G2/M arrest correlates well with the potency of aloisine A against CDK1/cyclin B.

Conclusion

In conclusion, we have identified 6-phenyl[5*H*]pyrrolo-[2,3-*b*]pyrazines (aloisines) as a new scaffold structure for protein kinase inhibition, active at submicromolar concentrations on cyclin-dependent kinases 1, 2, and 5. The excellent selectivity of these compounds for CDKs and for glycogen synthase kinase-3, two families of therapeutically relevant targets, is encouraging. The cocrystal structure of aloisine with CDK2 and the early structure/activity relationship studies provide some interesting clues to improve the potency of aloisines.

Experimental Section

Abbreviations. BSA, bovine serum albumin; CDK, cyclin-dependent kinase; DTT, dithiothreitol; GSK-3, glycogen synthase kinase-3; MTT, (4,5-dimethylthiazol-2-yl)-2,5-diphenyltetrazolium bromide; PBS, phosphate-buffered saline; TBS, Tris-buffered saline.
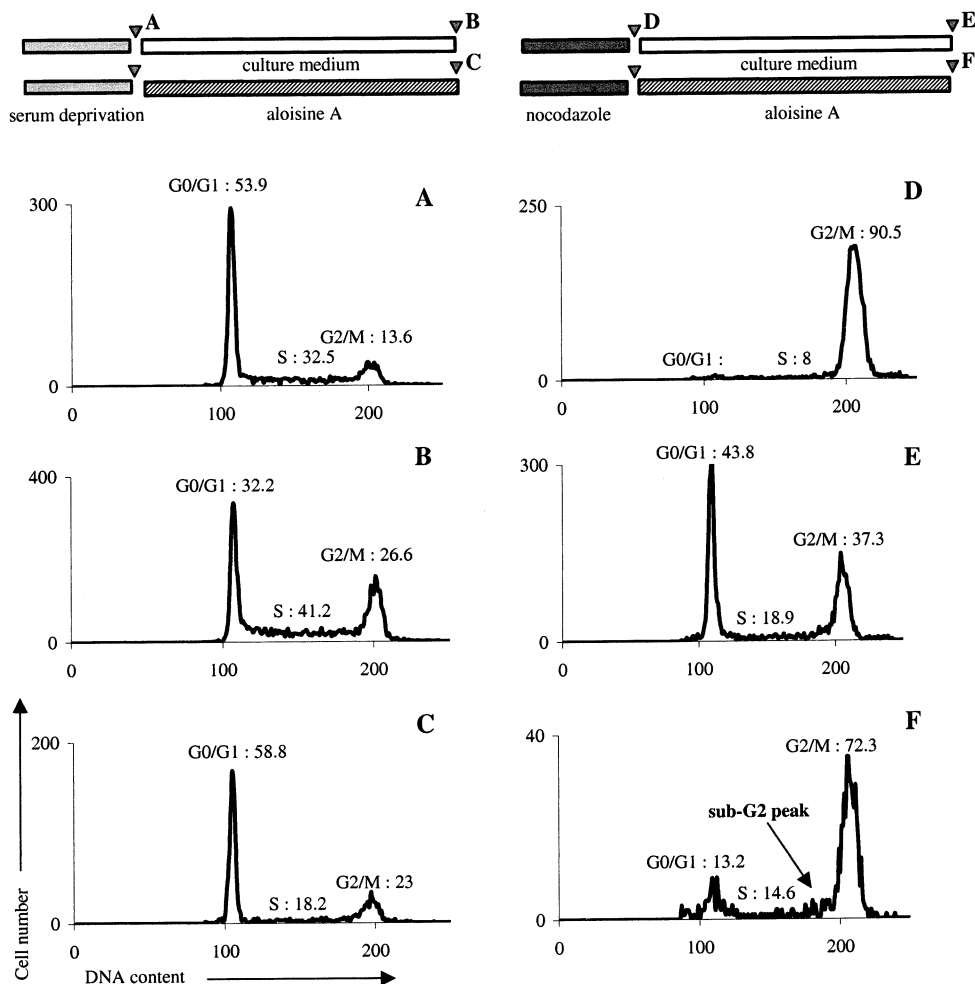
Figure 8. Comparison of the effects of aloisine A on G0/G1 (A–C) and G2/M (D–F) synchronized cells. The cell cycle phase distribution was analyzed by flow cytometry following propidium iodide staining. (A–C) NT2 cells were synchronized by serum deprivation for 24 h (A) and then cultured for 40 h in fresh medium without (B) or with 20 μM aloisine A (C). (D–F). NT2 cells were synchronized by nocodazole treatment (0.2 μg/mL) for 24 h (D) and then cultured for 40 h in fresh medium without (E) or with 20 μM aloisine A (F).

Chemistry. Melting points were measured in open capillary tubes on an Electrothermal 9200 apparatus and are uncorrected. IR spectra were taken in KBr on an ATI Mattson Genesis series FTIR. ^{1}H NMR spectra were recorded on a Varian EM 360 A spectrometer (60 MHz), and chemical shifts (ppm) are reported relative to tetramethylsilane. Signals are designated as follows: bs, broad singlet; s, singlet; d, doublet; dd, doublet of doublets; t, triplet; m, multiplet. Mass spectra were determined on an LKB 209 (EI at 70 eV). Elemental microanalyses are indicated by the symbol of the elements, and the results were within ±0.4% of the theoretical values unless otherwise stated; they were performed on a Perkin-Elmer 240 apparatus.

All experiments involving butyllithium or sodium hydride were carried out in dried apparatus under an atmosphere of dry, oxygen-free nitrogen. Tetrahydrofuran (THF) was distilled from benzophenone–sodium. Diisopropylamine and methyl heterocycles were distilled and stored over barium oxide. Butyllithium (1.6 M solution in hexane) was supplied by Acros and was assayed by titration against diphenylacetic acid. Alkyl- and aralkylpyrazines were prepared according to usual procedures. Grace silica gel 60 A, 20–45 μm, was employed for column chromatography. 2-Phenylindole was purchased from Aldrich and used as received.

General Method for the Synthesis of Aloisines. Diisopropylamine (2.23 g; 0.022 mol) in THF (50 mL) was cooled to 0 °C, and butyllithium (0.022 mol) was added dropwise. After being stirred for 30 min at 0 °C, the solution was cooled to −40 °C before addition of the heterocycle (0.02 mol) in THF (20 mL). After 30 min, the nitrile (0.01 mol) in THF (20 mL)

was added, and the solution was stirred for 30 min at −40 °C and further (1–20 h) at 20 °C, and then hydrolyzed with a 10% aqueous solution of NH$_4$Cl. The organic layer was dried over Na$_2$SO$_4$ and concentrated under vacuum. The crude product was chromatographed on silica gel and eluted with methylene chloride and then ethyl acetate. If necessary, the product was crystallized from ethanol or a methylene chloride–ethanol mixture.

6-(2-Furyl)[5*H*]pyrrolo[2,3-*b*]pyrazine (1, RP19): mp 232.6 °C; IR 3157, 3143, 3102 cm^{-1}; ^{1}H NMR (60 MHz, DMSO-d_6) δ 6.50–6.70 (m, 1H), 6.80 (s, 1H), 7.05 (d, 1H, J = 3 Hz), 7.80 (bs, 1H), 8.20 and 8.35 (2d, 1H each, J = 3 Hz), 12.45 (bs, 1H). Anal. (C$_{10}$H$_7$N$_3$O) C, H, N.

6-(2-Thienyl)[5*H*]pyrrolo[2,3-*b*]pyrazine (2, RP6): mp 260.3 °C; IR 3208, 3150, 3068 cm^{-1}; ^{1}H NMR (60 MHz, DMSO-d_6) δ 6.95 (bs, 1H), 7.15–7.45 (m, 1H), 7.75 (s, 1H), 7.85 (bd, 1H), 8.25 and 8.45 (2d, 1H each, J = 2.8 Hz), 12.85 (bs, 1H). Anal. (C$_{10}$H$_7$N$_3$S) C, H, N.

6-(3-Thienyl)[5*H*]pyrrolo[2,3-*b*]pyrazine (3, RP128): mp 230 °C dec; IR 3095, 3050, 3000 cm^{-1}; ^{1}H NMR (60 MHz, DMSO-d_6) δ 6.95 (s,1H), 7.60–7.75 (m, 2H), 8.10–8.20 (m, 2H), 8.30 (d, 1H, J = 2.6 Hz), 12.30 (bs, 1H). Anal. (C$_{10}$H$_7$N$_3$S) C, H, N.

6-(2-Pyridyl)[5*H*]pyrrolo[2,3-*b*]pyrazine (4, RP13): mp 233.1 °C; IR 3100, 3059 cm^{-1}; ^{1}H NMR (60 MHz, DMSO-d_6) δ 7.30–7.60 (m, 2H), 7.95–8.20 (m, 2H), 8.30 and 8.45 (2d, 1H each, J = 2.8 Hz), 8.75 (d, 1H, J = 5 Hz), 12.65 (bs, 1H). Anal. (C$_{11}$H$_8$N$_4$) C, H, N.

6-Phenyl[5*H*]pyrrolo[2,3-*b*]pyrazine (5, RP7): mp 216 °C (lit.[63] mp 215–216 °C); IR 3135, 3050 cm^{-1}; ^{1}H NMR (60

MHz, DMSO-d_6) δ 7.00 (s, 1H), 7.55 (m, 3H), 7.90 (m, 2H), 8.25 and 8.50 (2d, 1H each, J = 3 Hz), 11.90 (bs, 1H); MS m/e 209 (M$^+$, 100). Anal. (C$_{12}$H$_9$N$_3$) C, H, N.

6-(1-Naphthyl)[5*H*]pyrrolo[2,3-*b*]pyrazine (6, RP17): mp 216.4 °C; IR 3214, 3110, 3048 cm^{-1}; ^{1}H NMR (60 MHz, DMSO-d_6) δ 6.95 (s, 1H), 7.50−7.85 (m, 4H), 7.95−8.40 (m, 4H), 8.50 (d, 1H, J = 2.5 Hz), 12.05 (bs, 1H). Anal. (C$_{16}$H$_{11}$N$_3$) C, H, N.

6-Phenyl[5*H*]pyrrolo[2,3-*b*]quinoxaline (7, RP12): mp 260 °C dec (lit.[63] mp 233 °C dec); IR 3150 cm^{-1}; ^{1}H NMR (60 MHz, DMSO-d_6) δ 7.30 (s, 1H), 7.60 (m, 5H), 8.10 (m, 4H), 12.40 (bs, 1H). Anal. (C$_{16}$H$_{11}$N$_3$) C, H, N.

3-Methyl-6-phenyl[5*H*]pyrrolo[2,3-*b*]pyrazine (8, RP18): mp 261.8 °C; IR 3104, 3030, 2985, 2915, 2878, 2801 cm^{-1}; ^{1}H NMR (60 MHz, DMSO-d_6) δ 2.55 (s, 3H), 7.15 (s, 1H), 7.35−7.60 (m, 3H), 7.75−8.10 (m, 2H), 8.40 (s, 1H), 12.30 (bs, 1H); MS m/e 209 (M$^+$, 100). Anal. (C$_{13}$H$_{11}$N$_3$) C, H, N.

6-[1-(4-Chlorophenyl)-1-cyclopropyl][5*H*]pyrrolo[2,3-*b*]pyrazine (9, RP124): mp 189.7 °C; IR 3210, 3125, 3049, 3000, 2940, 2850 cm^{-1}; ^{1}H NMR (60 MHz, DMSO-d_6) δ 1.50 (d, 4H), 6.15 (s, 1H), 7.30 (s, 4H), 8.10 and 8.25 (2d, 1H each, J = 3 Hz), 12.00 (bs, 1H). Anal. (C$_{15}$H$_{12}$N$_3$Cl) C, H, N.

6-(2-Methoxyphenyl)[5*H*]pyrrolo[2,3-*b*]pyrazine (10, RP9): mp 156.9 °C; IR 3080, 3051, 2925, 2887, 2830 cm^{-1}; ^{1}H NMR (60 MHz, DMSO-d_6) δ 3.90 (s, 3H), 6.95−7.35 (m, 4H), 7.80−8.10 (m, 1H), 8.20 and 8.35 (2d, 1H each, J = 2.5 Hz), 11.90 (bs, 1H). Anal. (C$_{13}$H$_{11}$N$_3$O) C, H, N.

6-(3-Methoxyphenyl)[5*H*]pyrrolo[2,3-*b*]pyrazine (12, RP10): mp 195.7 °C; IR 3123, 2968, 2921, 2836 cm^{-1}; ^{1}H NMR (60 MHz, DMSO-d_6) δ 3.95 (s, 3H), 6.90−7.80 (m, 5H), 8.25 and 8.40 (2d, 1H each, J = 2.5 Hz), 12.55 (bs, 1H). Anal. (C$_{13}$H$_{11}$N$_3$O) C, H, N.

6-(4-Methoxyphenyl)[5*H*]pyrrolo[2,3-*b*]pyrazine (14, RP11): mp 256.1 °C (lit.[63] mp 238−240 °C dec); IR 3143, 3035, 2959, 2857 cm^{-1}; ^{1}H NMR (60 MHz, DMSO-d_6) δ 3.80 (s, 3H), 6.95−7.10 (m, 3H), 8.00 (d, 2H, J = 8 Hz), 8.15 and 8.35 (2d, 1H each, J = 2.6 Hz), 12.35 (bs, 1H). Anal. (C$_{13}$H$_{11}$N$_3$O) C, H, N.

6-(3,5-Dimethoxyphenyl)[5*H*]pyrrolo[2,3-*b*]pyrazine (16, RP21): mp 216.7 °C; IR 3150, 2950, 2880 cm^{-1}; ^{1}H NMR (60 MHz, DMSO-d_6) δ 3.90 (s, 6H), 6.55 (s, 1H), 7.20 (m, 3H), 8.15 and 8.35 (2d, 1H each, J = 2.5 Hz), 12.40 (bs, 1H). Anal. (C$_{14}$H$_{13}$N$_3$O$_2$) C, H, N.

6-(3,4,5-Trimethoxyphenyl)[5*H*]pyrrolo[2,3-*b*]pyrazine (17, RP16): mp 231.7 °C; IR 3098, 2964, 2939, 2834 cm^{-1}; ^{1}H NMR (60 MHz, DMSO-d_6) δ 3.75 (s, 3H), 3.95 (s, 6H), 7.25 (s, 1H), 7.40 (bs, 2H), 8.25 and 8.40 (2d, 1H each, J = 2 Hz), 12.45 (bs, 1H). Anal. (C$_{15}$H$_{15}$N$_3$O$_3$) C, H, N.

6-(4-Fluorophenyl)[5*H*]pyrrolo[2,3-*b*]pyrazine (18, RP76): mp 244 °C dec; IR 3149 cm^{-1}; ^{1}H NMR (60 MHz, DMSO-d_6) δ 7.05−7.50 (m, 3H), 7.65−8.10 (m, 2H), 8.20 and 8.35 (2d, 1H each, J = 2.4 Hz),12.45 (bs, 1H). Anal. (C$_{12}$H$_8$N$_3$F) C, H, N.

6-(4-Chlorophenyl)[5*H*]pyrrolo[2,3-*b*]pyrazine (19, RP14): mp 250 °C dec (lit.[63] mp 250 °C dec); IR 3300 cm^{-1}; ^{1}H NMR (60 MHz, DMSO-d_6) δ 7.20 (s, 1H), 7.55 and 8.05 (2d, 2H each, J = 8. Hz), 8.20 and 8.35 (2d, 1H each, J = 2.4 Hz), 12.45 (bs, 1H). Anal. (C$_{12}$H$_8$N$_3$Cl) C, H, N.

6-(3,5-Dichlorophenyl)[5*H*]pyrrolo[2,3-*b*]pyrazine (20, RP15): mp 252 °C dec; IR 3216, 3164, 3114 cm^{-1}; ^{1}H NMR (60 MHz, DMSO-d_6) δ 7.35 (s, 1H), 7.75 (m, 1H), 8.15 (d, 2H), 8.25 and 8.40 (2d, 1H each, J = 2.2 Hz), 12.40 (bs, 1H). Anal. (C$_{12}$H$_7$N$_3$Cl$_2$) C, H, N.

6-(4-Bromophenyl)[5*H*]pyrrolo[2,3-*b*]pyrazine (21, RP77): mp 256 °C dec; IR 3211, 3109 cm^{-1}; ^{1}H NMR (60 MHz, DMSO-d_6) δ 7.20 (s, 1H), 7.70 and 8.00 (2d, 2H each, J = 8.2 Hz), 8.20 and 8.35 (2d, 1H each, J = 2.5 Hz), 12.45 (bs, 1H). Anal. (C$_{12}$H$_8$N$_3$Br) C, H, N.

6-(4-Trifluoromethylphenyl)[5*H*]pyrrolo[2,3-*b*]pyrazine (22, RP8): mp 238 °C dec; IR 3164 cm^{-1}; ^{1}H NMR (60 MHz, DMSO-d_6) δ 7.35 (s, 1H), 7.85 (d, 2H, J = 8.2 Hz), 8.10−8.50 (m, 4H), 12.70 (bs, 1H). Anal. (C$_{13}$H$_8$N$_3$F$_3$) C, H, N.

6-(4-Cyanophenyl)[5*H*]pyrrolo[2,3-*b*]pyrazine (23, RP20): mp 340 °C dec; IR 3464, 3056, 2205 cm^{-1}; ^{1}H NMR (60 MHz, DMSO-d_6) δ 7.45 (s, 1H), 7.90−8.65 (m, 6H), 12.85 (bs, 1H). Anal. (C$_{13}$H$_8$N$_4$) C, H, N.

6-(4-Methylphenyl)[5*H*]pyrrolo[2,3-*b*]pyrazine (24, RP78): mp 265.4 °C; IR 3150, 3120, 2940, 2920 cm^{-1}; ^{1}H NMR (60 MHz, DMSO-d_6) δ 2.40 (s, 3H), 7.05 (s, 1H), 7.30 and 7.90 (2d, 2H each, J = 8 Hz), 8.15 and 8.30 (2d, 1H each, J = 2.4 Hz), 12.45 (bs, 1H). Anal. (C$_{13}$H$_{11}$N$_3$) C, H, N.

6-[4-(2-Dioxolyl)-phenyl][5*H*]pyrrolo[2,3-*b*]pyrazine (25, RP122): mp 265.6 °C; IR 3120, 2980, 2889 cm^{-1}; ^{1}H NMR (60 MHz, DMSO-d_6) δ 3.95 (s, 4H), 5.75 (s, 1H), 7.15 (s, 1H), 7.50 and 8.05, (2d, 2H each, J = 7 Hz), 8.20 and 8.35 (2d, 1H each, J = 3 Hz), 12.45 (bs, 1H). Anal. (C$_{15}$H$_{13}$N$_3$O$_2$) C, H, N.

6-(4-Dimethylaminophenyl)[5*H*]pyrrolo[2,3-*b*]pyrazine (26, RP129): mp 271 °C dec; IR 3211, 3157, 2900, 2818 cm^{-1}; ^{1}H NMR (60 MHz, DMSO-d_6) δ 3.15 (s, 6H), 6.80−6.90 (m, 3H), 7.85 (d, 2H, J = 8.Hz), 8.05 and 8.20 (2d, 1H each, J = 3 Hz), 12.15 (bs, 1H). Anal. (C$_{14}$H$_{14}$N$_4$) C, H, N.

6-(4-Methoxyphenyl)-7-methyl[5*H*]pyrrolo[2,3-*b*]pyrazine (27, RP95): mp 221.6 °C; IR 3142, 3043, 2955, 2844 cm^{-1}; ^{1}H NMR (60 MHz, DMSO-d_6) δ 2.40 (s, 3H), 3.80 (s, 3H), 7.10 and 7.70 (2d, 2H each, J = 7 Hz), 8.15 and 8.30 (2d, 1H each, J = 2.6 Hz), 12.00 (bs, 1H). Anal. (C$_{14}$H$_{13}$N$_3$O) C, H, N.

6-(3,4-Methoxyphenyl)-7-methyl[5*H*]pyrrolo[2,3-*b*]pyrazine (29, RP123): mp 230.2 °C; IR 3102, 2963, 2920, 2850 cm^{-1}; ^{1}H NMR (60 MHz, DMSO-d_6) δ 2.55 (s, 3H), 3.80 (s, 3H), 3.85 (s, 3H), 7.00−7.40 (m, 3H), 8.15 and 8.30 (2d, 1H each, J = 3 Hz), 12 (bs, 1H). Anal. (C$_{15}$H$_{15}$N$_3$O$_2$) C, H, N.

6-(4-Chlorophenyl)-7-methyl[5*H*]pyrrolo[2,3-*b*]pyrazine (30, RP80): mp 260 °C dec; IR 3148, 2920, 2853 cm^{-1}; ^{1}H NMR (60 MHz, DMSO-d_6) δ 2.40 (s, 3H), 7.40−7.85 (m, 4H), 8.15 and 8.30 (2d, 1H each, J = 2.5 Hz), 12.00 (bs, 1H). Anal. (C$_{13}$H$_{10}$N$_3$Cl) C, H, N.

6-(4-Dimethylaminosulfamoyloxyphenyl)-7-methyl[5*H*]pyrrolo[2,3-*b*]pyrazine (31, RP125): mp 235.1 °C; IR 3140, 3045, 2970, 2925, 2880 cm^{-1}; ^{1}H NMR (60 MHz, DMSO-d_6) δ 2.45 (s, 3H), 2.95 (s, 6H), 7.45 and 7.90 (2d, 2H each, J = 8 Hz), 8.30−8.50 (m, 2H), 12.25 (bs, 1H). Anal. (C$_{15}$H$_{16}$N$_4$SO$_3$) C, H, N.

6-(4-Methoxyphenyl)-7-propyl[5*H*]pyrrolo[2,3-*b*]pyrazine (32, RP127): mp 188.5 °C; IR 3215, 3158, 3055, 2958, 2934, 2866, 2836 cm^{-1}; ^{1}H NMR (60 MHz, DMSO-d_6) δ 0.9 (t, 3H, J = 7 Hz), 1.70 (m, 2H), 2.80 (t, 2H, J = 7 Hz), 3.80 (s, 3H), 7.05 and 7.65 (2d, 2H each, J = 8 Hz), 8.15 and 8.30 (2d, 1H each, J = 3 Hz), 12.00 (bs, 1H). Anal. (C$_{16}$H$_{17}$N$_3$O) C, H, N.

7-Allyl-6-(4-methoxyphenyl)[5*H*]pyrrolo[2,3-*b*]pyrazine (34, RP110): mp 193.8 °C; IR 3135, 3063, 2962, 2934, 2878, 2838 cm^{-1}; ^{1}H NMR (60 MHz, CDCl$_3$) δ 3.65−3.85 (m, 2H), 3.90 (s, 3H), 4.80−5.20 (m, 2H), 5.75−6.45 (m, 1H), 7.10 and 7.75 (2d, 2H each, J = 8.2 Hz), 8.05 and 8.40 (2d, 1H each, J = 2.4 Hz), 11.85 (bs, 1H). Anal. (C$_{16}$H$_{15}$N$_3$O) C, H, N.

7-(3-Chloropropyl)-6-(4-methoxyphenyl)[5*H*]pyrrolo[2,3-*b*]pyrazine (35, RP126): mp 178 °C dec; IR 3220, 3159, 3050, 3000, 2835 cm^{-1}; ^{1}H NMR (60 MHz, DMSO-d_6) δ 2.00−2.60 (m, 2H), 3.00 (m, 2H), 3.60 (t, 2H, J = 6 Hz), 3.80 (s, 3H), 7.10 and 7.70 (2d, 2H each, J = 8 Hz). 8.15 and 8.35 (2d, 1H each, J = 3 Hz), 12.00 (bs, 1H). Anal. (C$_{16}$H$_{16}$N$_3$OCl) C, H, N.

7-Isopropyl-6-(4-methoxyphenyl)[5*H*]pyrrolo[2,3-*b*]pyrazine (36, RP102): mp 204.8 °C; IR 3135, 3050, 2957, 2924, 2859 cm^{-1}; ^{1}H NMR (60 MHz, DMSO-d_6) δ 1.30 (d, 6H), 3.50 (m, 1H), 3.80 (s, 3H), 7.10 and 7.55 (2d, 2H each, J = 8 Hz), 8.15 and 8.35 (2d, 1H each, J = 2.4 Hz), 11.75 (bs, 1H). Anal. (C$_{16}$H$_{17}$N$_3$O) C, H, N.

6-(4-Chlorophenyl)-7-isopropyl[5*H*]pyrrolo[2,3-*b*]pyrazine (37, RP90): mp 208.6 °C; IR 3130, 3051, 2977, 2925, 2869 cm^{-1}; ^{1}H NMR (60 MHz, CDCl$_3$) δ 1.50 (d, 6H, J = 6 Hz), 3.25 (m, 1H), 7.60 (s, 4H), 8.20 and 8.35 (2d, 1H each, J = 2.5 Hz), 12.00 (bs, 1H). Anal. (C$_{15}$H$_{14}$N$_3$Cl) C, H, N.

7-*n*-Butyl-6-(4-methoxyphenyl)[5*H*]pyrrolo[2,3-*b*]pyrazine (38, RP106): mp 183.8 °C; IR 3143, 3050, 2956, 2934, 2870 cm^{-1}; ^{1}H NMR (60 MHz, DMSO-d_6) δ 1.00 (t, 3H, J = 7.2 Hz), 1.60 (m, 4H), 3.00 (t, 2H, J = 7.6 Hz), 3.90 (s, 3H), 7.10 and 7.70 (2d, 2H each, J = 8 Hz), 8.00 and 8.30 (2d, 1H each, J = 2.6 Hz), 11.75 (bs, 1H). Anal. (C$_{17}$H$_{19}$N$_3$O) C, H, N.

7-*n*-Butyl-6-(4-chlorophenyl)[5*H*]pyrrolo[2,3-*b*]pyrazine (40, RP108): mp 200 °C; IR 3161, 3048, 2954, 2924, 2856 cm^{-1}; ^{1}H NMR (60 MHz, DMSO-d_6) δ 0.90 (t, 3H, $J = 6$ Hz), 1.20−2.00 (m, 4H), 2.95 (t, 2H, $J = 7.2$ Hz), 7.65 (s, 4H), 8.25 and 8.40 (2d, 1H each, $J = 2.5$ Hz), 12.05 (bs, 1H). Anal. (C$_{16}$H$_{16}$N$_3$Cl) C, H, N.

7-*n*-Heptyl-6-(4-methoxyphenyl)[5*H*]pyrrolo[2,3-*b*]pyrazine (41, RP111): mp 132.5 °C; IR 3142, 3064, 2955, 2925, 2850 cm^{-1}; ^{1}H NMR (60 MHz, CDCl$_3$) δ 0.90−2.00 (m, 13H), 3.05 (t, 2H, $J = 7.2$ Hz), 3.90 (s, 3H), 7.05 and 7.70 (2d, 2H each, $J = 8.2$ Hz), 8.00 and 8.40 (2d, 1H each, $J = 3$ Hz), 12.05 (bs, 1H). Anal. (C$_{20}$H$_{25}$N$_3$O) C, H, N.

6-(4-Methoxyphenyl)-7-methylcyclopropyl[5*H*]pyrrolo[2,3-*b*]pyrazine (42, RP104): mp 193.9 °C; IR 3142, 3080, 3046, 3000, 2931, 2820 cm^{-1}; ^{1}H NMR (60 MHz, DMSO-d_6) δ 0.20−0.50 (m, 4H), 1.00−1.40 (m, 1H), 2.90 (d, 2H, $J = 6$ Hz), 3.85 (s, 3H), 7.15 and 7.75 (2d, 2H each, $J = 8.2$ Hz), 8.20 and 8.40 (2d, 1H each, $J = 2.6$ Hz), 12.20 (bs, 1H). Anal. (C$_{17}$H$_{17}$N$_3$O) C, H, N.

7-Benzyl-6-phenyl[5*H*]pyrrolo[2,3-*b*]pyrazine (44, RP92): mp 209.8 °C; IR 3144, 3056, 3024, 2929, 2871 cm^{-1}; ^{1}H NMR (60 MHz, DMSO-d_6) δ 4.30 (s, 2H), 7.20 (s, 6H), 7.75−8.25 (m, 4H), 8.30 and 8.40 (2d, 1H each, $J = 3$ Hz), 12.25 (bs, 1H). Anal. (C$_{19}$H$_{15}$N$_3$) C, H, N.

7-Benzyl-6-(4-chlorophenyl)[5*H*]pyrrolo[2,3-*b*]pyrazine (45, RP91): mp 266.3 °C; IR 3138, 3050, 3025, 2928, 2858 cm^{-1}; ^{1}H NMR (60 MHz, DMSO-d_6) δ 4.25 (s, 2H), 7.15 (s, 5H), 7.55 (s, 4H), 8.20 and 8.35 (2d, 1H each, $J = 3$ Hz), 12.25 (bs, 1H). Anal. (C$_{19}$H$_{14}$N$_3$Cl) C, H, N.

6-(4-Methoxyphenyl)-7-methylcyclohexyl[5*H*]pyrrolo[2,3-*b*]pyrazine (46, RP98): mp 220.3 °C; IR 3434, 3135, 2921, 2850 cm^{-1}; ^{1}H NMR (60 MHz, DMSO-d_6) δ 0.85−1.80 (m, 11H), 2.80 (d, 2H, $J = 6.5$ Hz), 3.80 (s, 3H), 7.15 and 7.70 (2d, 2H each, $J = 8.2$ Hz), 8.15 and 8.35 (2d, 1H each, $J = 2.5$ Hz), 11.90 (bs, 1H). Anal. (C$_{20}$H$_{23}$N$_3$O) C, H, N.

6-(4-Chlorophenyl)-7-methylcyclohexyl[5*H*]pyrrolo[2,3-*b*]pyrazine (47, RP99): mp 203.5 °C; IR 3142, 3048, 2928, 2847 cm^{-1}; ^{1}H NMR (60 MHz, DMSO-d_6) δ 0.80−1.75 (m, 11H), 2.80 (d, 2H, $J = 6.5$ Hz), 7.65 (s, 4H), 8.20 and 8.40 (2d, 1H each, $J = 2.4$ Hz), 12.10 (bs, 1H). Anal. (C$_{19}$H$_{20}$N$_3$Cl) C, H, N.

5-Methyl-6-phenylpyrrolo[2,3-*b*]pyrazine (48, RP22): mp 72.3 °C; IR 3100, 3051, 2948 cm^{-1}; ^{1}H NMR (60 MHz, DMSO-d_6) δ 3.75 (s, 3H), 6.70 (s, 1H), 7.45 (s, 5H), 8.20 and 8.40 (2d, 1H each, $J = 2.4$ Hz). Anal. (C$_{13}$H$_{11}$N$_3$) C, H, N.

6-[1-(4-Chlorophenyl)-1-cyclopropyl]-7-methyl[5*H*]pyrrolo[2,3-*b*]pyrazine (49, RP130): mp 223.9 °C; IR 3135, 3055, 2921, 2857, 2780 cm^{-1}; ^{1}H NMR (60 MHz, DMSO-d_6) δ 1.40 (s, 4H), 2.30 (s, 3H), 7.30 (bs, 4H), 8.20 and 8.35 (2d, 1H each, $J = 2.8$ Hz), 11.95 (bs, 1H). Anal. (C$_{16}$H$_{14}$N$_3$Cl) C, H, N.

2-(4-Methoxyphenyl)[1*H*]pyrrolo[2,3-*b*]pyridine (50, RP97): mp 206.2 °C; IR 3143, 2930, 2846, cm^{-1}; ^{1}H NMR (60 MHz, DMSO-d_6) δ 3.45 (s, 3H), 6.75 (s, 1H), 6.90−7.15 (m, 3H), 7.70−7.95 (m, 3H), 8.15 (d, 1H, $J = 4$ Hz), 11.95 (s, 1H). Anal. (C$_{14}$H$_{12}$N$_2$O) C, H, N.

General Method for the Demethylation of Methoxy-Substituted 6-Phenyl[5*H*]pyrrolo[2,3-*b*]pyrazines. First, hydrobromidic acid was redistilled over a trace of 50% hypophosphorous acid: 1 g for each 100 g of 48% hydrobromidic acid. Methoxy compound (0.003 mol) was heated with hydrobromidic acid (20 mL). After removal of the aqueous forerun, the temperature reached 126 °C. The time required for demethylation varied from 3 to 10 h. The excess hydrobromidic acid was removed under reduced pressure, and the crude product was crystallized from ethanol.

6-(2-Hydroxyphenyl)[5*H*]pyrrolo[2,3-*b*]pyrazine hydrobromide (11, RP109): mp 250 °C dec; IR 3419, 3354, 3090, 2710, 2641 cm^{-1}; ^{1}H NMR (60 MHz, DMSO-d_6) δ 5.80 (s, 3H), 6.80−7.30 (m, 4H), 7.70−8.00 (m, 1H), 8.40 (bs, 3H), 12.85 (bs, 1H). Anal. (C$_{12}$H$_9$N$_3$O, HBr, H$_2$O) C, H, N.

6-(3-Hydroxyphenyl)[5*H*]pyrrolo[2,3-*b*]pyrazine hydrobromide (13, RP134): mp 258 °C dec; IR 3448, 3137, 3085, 2700, 2630 cm^{-1}; ^{1}H NMR (60 MHz, DMSO-d_6) δ 6.70−

7.50 (m, 7H), 8.65 (bs, 2H), 13.45 (bs, 1H). Anal. (C$_{12}$H$_9$N$_3$O, HBr) C, H, N.

6-(4-Hydroxyphenyl)[5*H*]pyrrolo[2,3-*b*]pyrazine hydrobromide (15, RP26): mp 255 °C dec; IR 3448, 3176, 3060 cm^{-1}; ^{1}H NMR (60 MHz, DMSO-d_6) δ 6.65−6.85 (m, 4H), 7.70 and 7.85 (2d, 2H each, $J = 8.2$ Hz), 8.15 and 8.25 (2d, 1H each, $J = 3$ Hz), 9.65 (s, 1H), 12.10 (bs, 1H). Anal. (C$_{12}$H$_9$N$_3$O, HBr, H$_2$O) C, H, N.

6-(4-Hydroxyphenyl)-7-methyl[5*H*]pyrrolo[2,3-*b*]pyrazine hydrobromide (28, RP96): mp 262 °C dec; IR 3465, 3143, 3090, 2796, 2759 cm^{-1}; ^{1}H NMR (60 MHz, DMSO-d_6) δ 2.45 (s, 3H), 7.00 and 7.70 (2d, 2H each, $J = 8.2$ Hz), 8.50 (bs, 2H), 9.80 (s, 2H), 13.00 (bs, 1H). Anal. (C$_{13}$H$_{11}$N$_3$O, HBr) C, H, N.

6-(4-Hydroxyphenyl)-7-propyl[5*H*]pyrrolo[2,3-*b*]pyrazine hydrobromide (33, RP132): mp 244 °C dec; IR 3187, 3100, 2965, 2873, 2798 cm^{-1}; ^{1}H NMR (60 MHz, DMSO-d_6) δ 0.85 (t, 3H, $J = 7$ Hz), 1.35−1.90 (m, 2H), 3.10−2.75 (m, 2H), 7.20 and 7.65 (2d, 2H each, $J = 8.2$ Hz), 8.50 (s, 2H), 9.8 (s, 2H), 13.1 (s, 1H). Anal. (C$_{15}$H$_{15}$N$_3$O, HBr) C, H, N.

7-*n*-Butyl-6-(4-hydroxyphenyl)[5*H*]pyrrolo[2,3-*b*]pyrazine (39, RP107): mp 281.4 °C; IR 3134, 3100, 2946, 2924, 2867 cm^{-1}; ^{1}H NMR (60 MHz, DMSO-d_6) δ 0.90 (t, 3H, $J = 7$ Hz), 1.20−1.90 (m 4H), 2.90 (t, 2H, $J = 7.5$ Hz), 6.95 and 7.60 (2d, 2H each, $J = 7$ Hz), 8.15 and 8.30 (2d, 1H each, $J = 2.6$ Hz), 9.80 (bs, 1H), 11.80 (bs, 1H). Anal. (C$_{16}$H$_{17}$N$_3$O) C, H, N.

6-(4-Hydroxyphenyl)-7-methylcyclopropyl[5*H*]pyrrolo[2,3-*b*]pyrazine hydrobromide (43, RP112): mp 260 °C dec; IR 3482, 3335, 3064, 2983 cm^{-1} ; ^{1}H NMR (60 MHz, DMSO-d_6) δ 1.60 (d, 4H, $J = 6$ Hz), 2.00−2.60 (m, 3H), 2.90−3.60 (m, 4H), 7.05 and 7.90 (2d, 2H each, $J = 8.2$ Hz), 8.55−8.80 (m, 2H), 13.45 (bs, 1H). Anal. (C$_{16}$H$_{15}$N$_3$O, HBr, H$_2$O) C, H, N.

Biochemistry. (a) Biochemical Reagents. Sodium orthovanadate, EGTA, EDTA, Mops, β-glycerophosphate, phenyl phosphate, sodium fluoride, dithiothreitol (DTT), glutathione agarose, glutathione, bovine serum albumin (BSA), nitrophenyl phosphate, leupeptin, aprotinin, pepstatin, soybean trypsin inhibitor, benzamidine, and histone H1 (type III-S) were obtained from Sigma Chemicals. [γ-^{32}P]ATP (PB 168) was obtained from Amersham. The GS-1 peptide (YRRAAVPP-SPSLSRHSSPHQSpEDEEE) was synthesized by the Peptide Synthesis Unit, Institute of Biomolecular Sciences, University of Southampton, Southampton SO16 7PX, U.K.

(b) Buffers. 1. Homogenization buffer: 60 mM β-glycerophosphate, 15 mM *p*-nitrophenyl phosphate, 25 mM Mops (pH 7.2), 15 mM EGTA, 15 mM MgCl$_2$, 1 mM DTT, 1 mM sodium vanadate, 1 mM NaF, 1 mM phenyl phosphate, 10 μg of leupeptin/mL, 10 μg of aprotinin/mL, 10 μg of soybean trypsin inhibitor/mL, and 100 μM benzamidine.

2. Buffer A: 10 mM MgCl$_2$, 1 mM EGTA, 1 mM DTT, 25 mM Tris-HCl (pH 7.5), 50 μg of heparin/mL.

3. Buffer C: same as homogenization buffer but with 5 mM EGTA, no NaF, and no protease inhibitors.

4. Tris-buffered saline−Tween-20 (TBST): 50 mM Tris (pH 7.4), 150 mM NaCl, 0.1% Tween-20.

5. Hypotonic lysis buffer (HLB): 50 mM Tris-HCl (pH 7.4), 120 mM NaCl, 10% glycerol, 1% Nonidet-P40, 5 mM DTT, 1 mM EGTA, 20 mM NaF, 1 mM orthovanadate, 5 μM microcystin, 100 μg/mL each of leupeptin, aprotinin, and pepstatin.

(c) Kinase Preparations and Assays. Kinases activities were assayed in buffer A or C (unless otherwise stated), at 30 °C, at a final ATP concentration of 15 μM. Blank values were subtracted and activities calculated as picomoles of phosphate incorporated for a 10-min incubation. The activities are usually expressed in percent of the maximal activity, i.e., in the absence of inhibitors. Controls were performed with appropriate dilutions of dimethyl sulfoxide. In a few cases, phosphorylation of the substrate was assessed by autoradiography after SDS−PAGE.

GSK-3β was either purified from porcine brain or expressed in and purified from insect Sf9 cells.[32] It was assayed, following a 1/100 dilution in 1 mg of BSA/mL of 10 mM DTT, with 5 μL of 40 μM GS-1 peptide as a substrate, in buffer A, in the

presence of 15 μM [γ-^{32}P]ATP (3000 Ci/mmol; 1 mCi/mL) in a final volume of 30 μl. After 30 min of incubation at 30 °C, 25-μL aliquots of supernatant were spotted onto 2.5- × 3-cm pieces of Whatman P81 phosphocellulose paper, and 20 s later, the filters were washed five times (for at least 5 min each time) in a solution of 10 mL of phosphoric acid/L of water. The wet filters were counted in the presence of 1 mL of ACS (Amersham) scintillation fluid.

CDK1/cyclin B was extracted in homogenization buffer from M phase starfish (*Marthasterias glacialis*) oocytes and purified by affinity chromatography on p9^{CKShs1}-sepharose beads, from which it was eluted by free p9^{CKShs1} as previously described.[32,35] The kinase activity was assayed in buffer C, with 1 mg of histone H1/mL, in the presence of 15 μM [γ-^{32}P]ATP (3000 Ci/mmol; 1 mCi/mL) in a final volume of 30 μL. After 10 min of incubation at 30 °C, 25-μL aliquots of supernatant were spotted onto P81 phosphocellulose papers and treated as described above.

CDK5/p25 was reconstituted by mixing equal amounts of recombinant mammalian CDK5 and p25 expressed in *E. coli* as GST (glutathione-S-transferase) fusion proteins and purified by affinity chromatography on glutathione agarose (vectors kindly provided by Dr. J. H. Wang) (p25 is a truncated version of p35, the 35 kDa CDK5 activator). Its activity was assayed in buffer C as described for CDK1/cyclin B.

Other kinases were expressed, purified, and assayed as described previously.[20,37]

Crystallography. (a) Expression, Purification, and Crystallization of Human CDK2. Human CDK2 was expressed from a recombinant baculovirus in Sf9 insect cells and purified according to slightly modified published method.[74,75] Monomeric unphosphorylated CDK2 crystals were grown as previously described.[68]

(b) X-ray Crystallography Data Collection and Processing. The CDK2−aloisine B dataset was collected from a monomeric CDK2 crystal soaked for 60 h in 1 mM aloisine B in 1× mother liquor solution (50 mM ammonium acetate, 10% PEG3350, 15 mM NaCl, 100 mM HEPES, pH 7.4) plus 5% DMSO. Data were collected on beamline X-RAY DIFFRACTION at the Elettra Light Source at 100K after the crystal had been transferred briefly to cryoprotectant (mother liquor adjusted to contain 20% glycerol). The images were integrated with the MOSFLM package,[76] and reflections were subsequently scaled and merged using SCALA.[77] Subsequent data reduction and structure refinement were pursued through programs of the CCP4 suite.[77] Statistics of the datasets used in the structure determination are given in Table 6.

(c) Structure Solution and Refinement. The starting model for CDK2 refinement was a 1.3-Å resolution model of CDK2 in complex with an O6-substituted guanine derivative (unpublished data). The positioning of this search model in our isomorphous crystals was confirmed by molecular replacement using AMoRE.[78] Refinement was begun by carrying out rigid body refinement of the structure using REFMAC[79] and using sequentially higher resolution data. As the resolution of the data included was increased from 3.0 to 1.9 Å, increasing numbers of rigid bodies were used, so that initially the whole molecule was treated as a single rigid body, and finally individual secondary structural elements were allowed to refine independently. Following rigid body refinement, the (F_o - F_c)α_{calc} maps included readily interpretable electron density for the bound inhibitor. The structure was then compared with $2F_o - F_c$ electron density maps using the program "O",[80] and minor structural changes were introduced. Following the first round of model building, a model of aloisine B generated within the CCP4 molecular sketcher[77] was built into the electron density map and included in subsequent refinement steps. Refinement was then pursued with alternating cycles of interactive model building and maximum likelihood refinement using REFMAC. Toward the end of the refinement, water molecules were added using the program ARP.[81] Structure refinement was completed when addition of further waters, or the rebuilding of the disordered loops, resulted in no

improvement in the value of R_{free}. Statistics of the final models are given in Table 6.

The analysis of the surface area involved in the CDK2−aloisine B complex was carried out using the program Aesop (M.N., unpublished). Atomic radii were taken from a database of unified atom values, and a solvent probe radius of 1.4 Å was used.

Cell Biology. (a) Reagents. Penicillin, streptomycin, nocodazole, insulin, transferrin, progesterone, putrescine, sodium selenite, 3-(4,5-dimethylthiazol-2-yl)-2,5-diphenyltetrazolium bromide (MTT), RNAse A, and propidium iodide were purchased from Sigma.

(b) Cell Cultures. Clonal human NT2 teratocarcinoma cells were obtained from Stratagene (La Jolla, CA) and grown in Dulbecco's Modified Eagle Medium Nutrient Mixture F-12 with 2 mM l-glutamine (BIO WHITTAKER) supplemented with 5% FCS and containing penicillin (20 IU/mL) and streptomycin (20 μg/mL) at 37 °C, in a humidified atmosphere containing 5% CO$_2$ in air.

(c) NT2 Differentiation. Differentiation of hNT cells from NT2 cells was induced according to the method of Pleasure et al.,[82] modified by Soulié et al. (submitted). Briefly, after the second replating, cells were cultured in serum-free medium with a combination of mitotic inhibitors (1 μM cytosine arabinoside, 10 μM fluorodeoxyuridine, and 10 μM uridine) and a mixture of salt and hormones (25 μg of insulin/mL, 100 μg of transferrin/mL, 20 nM progesterone, 60 μM putrescine, and 30 nM sodium selenite) for 5 days before treatment.

(d) Treatment with Aloisine. Exponentially growing cells were incubated for 24 h with aloisine A (stock solution dissolved in dimethyl sulfoxide). Nocodazole treatment of cells was performed at a concentration of 0.04 μg of nocodazole/mL of medium for 24 h. Following the nocodazole treatment, cells were washed twice with fresh medium and cultured with or without aloisine A for 24 h. To perform serum deprivation, cells were maintained in serum-free medium for 40 h. Following serum deprivation, cells were washed twice and cultured in fresh serum-containing medium with or without aloisine A for 40 h.

(e) Cell Viability Assay. To quantify the toxicity of aloisine A on NT2 cells and hNT human neurons, we measured the inhibition of cellular reduction of MTT to MTT formazan according to Saillé et al.[83] Following aloisine A exposure, cells were incubated with 0.5 mg of MTT/mL of fresh medium at 37 °C for 1 h. The formazan products were dissolved in DMSO and quantified by measurement of the absorbance at 562 nm.

(f) Cell Cycle Analysis by Flow Cytometry. Cells were trypsinized, collected by centrifugation, and fixed in cold 70% ethanol for at least 4 h. Fixed cells were washed in PBS, incubated with 10 μg of RNAse A/mL, and stained with 25 μg of propidium iodide/mL for 1 h at 37 °C. The stained cells were then analyzed for cell cycle distribution on a FACSort flow cytometer (Becton Dickinson). Cell cycle analyzes were performed as described[84] using multiCYCLE (P Rabanovitch).

References

(1) Adams, J. L.; Lee, D. Recent progress towards the identification of selective inhibitors of serine/threonine protein kinases. *Curr. Opin. Drug Discovery Dev.* **1999**, *2*, 96−109.

(2) Garcia-Echeverria, C.; Traxler, P.; Evans, D. B. ATP site-directed competitive and irreversible inhibitors of protein kinases. *Med. Res. Rev.* **2000**, *20*, 28−57.

(3) Sridhar, R.; Hanson-Painton, O.; Cooper, D. R. Protein kinases as therapeutic targets. *Pharm. Res.* **2000**, *17*, 1345−1353.

(4) Dumas, J. Protein kinase inhibitors: emerging pharmacophores 1997−2000. *Exp. Opin. Ther. Patents* **2001**, *11*, 405−429.

(5) Morgan, D. O. Cyclin-dependent kinases: engines, clocks, and microprocessors. *Annu. Rev. Cell. Dev. Biol.* **1997**, *13*, 261−291.

(6) Pavletich, N. P. Mechanisms of cyclin-dependent kinase regulation: structures of cdks, their cyclin activators, and Cip and INK4 inhibitors. *J. Mol. Biol.* **1999**, *287*, 821−828.

(7) Malumbres, M.; Ortega, S.; Barbacid, M. Genetic analysis of mammalian cyclin-dependent kinases and their inhibitors. *Biol. Chem.* **2000**, *381*, 827−838.

(8) Nikolic, M.; Tsai, L. H. Activity and regulation of p35/Cdk5 kinase complex. *Methods Enzymol.* **2000**, *325*, 200−213.

(9) Maccioni, R. B.; Otth, C.; Concha, I. I.; Munoz, J. P. The protein kinase Cdk5. Structural aspects, roles in neurogenesis and involvement in Alzheimer's pathology. *Eur. J. Biochem.* **2001**, *268*, 1518−1527.

(10) Dhavan, R.; Tsai, L.-H. A decade of CDK5. *Nature Rev. Mol. Cell Biol.* **2001**, *2*, 749−759.

(11) Malumbres, M.; Barbacid, M. To cycle or not to cycle: a critical decision in cancer. *Nature Rev. Cancer* **2001**, *1*, 222−231.

(12) Dominguez, I.; Green, J. B. Missing links in GSK3 regulation. *Dev. Biol.* **2001**, *15*, 303−313.

(13) Harwood, A. J. Regulation of GSK-3: a cellular multiprocessor. *Cell* **2001**, *29*, 821−824.

(14) Cohen, P.; Frame, S. The renaissance of GSK3. *Nature Rev. Mol. Cell Biol.* **2001**, *2*, 769−776.

(15) Frame, S.; Cohen, P. GSK3 takes center stage more than 20 years after its discovery. *Biochem. J.* **2001**, *359*, 1−16.

(16) Grimes, C. A.; Jope, R. S. The multifaceted roles of glycogen synthase kinase 3 in cellular signaling. *Prog. Neurobiol.* **2001**, *65*, 391−426.

(17) Eldar-Finkelman, H. Glycogen synthase kinase 3: an emerging therapeutic target. *Trends Mol. Med.* **2002**, *8*, 126−132.

(18) Knockaert, M.; Greengard, P.; Meijer, L. Pharmacological inhibitorsof cyclin-dependent kinases. *Trends Pharmacol. Sci.* **2002**, *23*, 417−425.

(19) Vesely, J.; Havlicek, L.; Strnad, M.; Blow, J. J.; Donella-Deana, A.; Pinna, L.; Letham, D. S.; Kato, J. Y.; Détivaud, L.; Leclerc, S.; Meijer, L. Inhibition of cyclin-dependent kinases by purine derivatives. *Eur. J. Biochem.* **1994**, *224*, 771−786.

(20) Meijer, L.; Borgne, A.; Mulner, O.; Chong, J. P. J.; Blow, J. J.; Inagaki, N.; Inagaki, M.; Delcros, J. G.; Moulinoux, J. P. Biochemical and cellular effects of roscovitine, a potent and selective inhibitor of the cyclin-dependent kinases cdc2, cdk2 and cdk5. *Eur. J. Biochem.* **1997**, *243*, 527−536.

(21) de Azevedo, W. F.; Leclerc, S.; Meijer, L.; Havlicek, L.; Strnad, M.; Kim, S. H. Inhibition of cyclin-dependent kinases by purine analogues: crystal structure of human cdk2 complexed with roscovitine. *Eur. J. Biochem.* **1997**, *243*, 518−526.

(22) Gray, N.; Wodicka, L.; Thunnissen, A. M.; Norman, T.; Kwon, S.; Espinoza, F. H.; Morgan, D. O.; Barnes, G.; Leclerc, S.; Meijer, L.; Kim, S. H.; Lockhart, D. J.; Schultze, P. Exploiting chemical libraries, structure, and genomics in the search for new kinase inhibitors. *Science* **1998**, *281*, 533−538.

(23) Chang, Y. T.; Gray, N. S.; Rosania, G. R.; Sutherlin, D. P.; Kwon, S.; Norman, T. C.; Sarohia, R.; Leost, M.; Meijer, L.; Schultz, P. G. Synthesis and application of functionally diverse 2,6,9-trisubstituted purine libraries as CDK inhibitors. *Chem. Biol.* **1999**, *6*, 361−375.

(24) Brooks, E. E.; Gray, N. S.; Joly, A.; Kerwar, S. S.; Lum, R.; Mackman, R. L.; Norman, T. C.; Rosete, J.; Rowe, M.; Schow, S. R.; Schultz, P. G.; Wang, X.; Wick, M. M.; Shiffman, D. CVT-313, a specific and potent inhibitor of CDK2 that prevents neointimal proliferation. *J. Biol. Chem.* **1997**, *272*, 29207−29211.

(25) Legraverend, M.; Noble, M.; Tunnah, P.; Ducrot, P.; Ludwig, O.; Leclerc, S.; Grierson, D. S.; Meijer, L.; Endicott, J. Cyclin-dependent kinase inhibition by new C-2 alkylynated purine derivatives and molecular structure of a CDK2−inhibitor complex. *J. Med. Chem.* **2000**, *43*, 1282−1292.

(26) Dreyer, M. K.; Borcherding, D. R.; Dumont, J. A.; Peet, N. P.; Tsay, J. T.; Wright, P. S.; Bitonti, A. J.; Shen, J.; Kim, S. H. Crystal structure of human cyclin-dependent kinase 2 in complex with the adenine-derived inhibitor H717. *J. Med. Chem.* **2001**, *44*, 524−530.

(27) Arris, C. E.; Boyle, F. T.; Calvert, A. H.; Curtin, N. J.; Endicott, J. A.; Garman, E. F.; Gibson, A. E.; Golding, B. T.; Grant, B. T.; Griffin, R. J.; Jewsbury, P.; Johnson, L. N.; Lawrie, A. M.; Newell, D. R.; Noble, M. E. M.; Sausville, E. A.; Schultz, R.; Yu, W. Identification of novel purine and pyrimidine cycline-dependent kinase inhibitors with distinct molecular interactions and tumor cell growth inhibition profiles. *J. Med. Chem.* **2000**, *43*, 2797−2804.

(28) Shum, P. W.; Peet, N. P.; Weintraub, P. M.; Le, T. B.; Zhao, Z.; Barbone, F.; Cashman, B.; Tsay, J.; Dwyer, S.; Loos, P. C.; Powers, E. A.; Kropp, K.; Wright, P. S.; Bitonti, A.; Dumont, J.; Borcherding, D. R. The design and synthesis of purine inhibitors of CDK2. III. *Nucleosides Nucleotides Nucleic Acids* **2001**, *20*, 1067−1078.

(29) Park, S. G.; Cheon, J. Y.; Lee, Y. H.; Park, J. S.; Lee, K. Y.; Lee, C. H.; Lee, S. K. A specific inhibitor of cyclin-dependent protein kinases, CDC2 and CDK2. *Mol. Cells* **1996**, *6*, 679−683.

(30) Sedlacek, H. H. Mechanism of action of flavopiridol. *Crit. Rev. Oncol./Hematol.* **2001**, *38*, 139−170.

(31) Hoessel, R.; Leclerc, S.; Endicott, J.; Noble, M.; Lawrie, A.; Tunnah, P.; Leost, M.; Damiens, E.; Marie, D.; Marko, D.; Niederberger, E.; Tang, W.; Eisenbrand, G.; Meijer, L. Indirubin, the active constituent of a Chinese antileukaemia medicine, inhibits cyclin-dependent kinases. *Nature Cell Biol.* **1999**, *1*, 60−67.

(32) Leclerc, S.; Garnier, M.; Hoessel, R.; Marko, D.; Bibb, J. A.; Snyder, G. L.; Greengard, P.; Biernat, J.; Mandelkow, E.-M.; Eisenbrand, G.; Meijer, L. Indirubins inhibit glycogen synthase kinase-3β and CDK5/p25, two kinases involved in abnormal tau phosphorylation in Alzheimer's disease—A property common to most CDK inhibitors? *J. Biol. Chem.* **2001**, *276*, 251−260.

(33) Schultz, C.; Link, A.; Leost, M.; Zaharevitz, D. W.; Gussio, R.; Sausville, E. A.; Meijer, L.; Kunick, C. The paullones, a series of cyclin-dependent kinase inhibitors: synthesis, evaluation of CDK1/cyclin B inhibition, and in vitro antitumor activity. *J. Med. Chem.* **1999**, *42*, 2909−2919.

(34) Zaharevitz, D.; Gussio, R.; Leost, M.; Senderowicz, A. M.; Lahusen, T.; Kunick, C.; Meijer, L.; Sausville, E. A. Discovery and initial characterization of the paullones, a novel class of small-molecule inhibitors of cyclin-dependent kinases. *Cancer Res.* **1999**, *59*, 2566−2569.

(35) Leost, M.; Schultz, C.; Link, A.; Wu, Y.-Z.; Biernat, J.; Mandelkow, E.-M.; Bibb, J. A.; Snyder, G. L.; Greengard, P.; Zaharevitz, D. W.; Gussio, R.; Senderovitz, A.; Sausville, E. A.; Kunick, C.; Meijer, L. Paullones are potent inhibitors of glycogen synthase kinase-3β and cyclin-dependent kinase 5/p25. *Eur. J. Biochem.* **2000**, *267*, 5983−5994.

(36) Kitagawa, M.; Okabe, T.; Ogino, H.; Matsumoto, H.; Suzuki-Takahashi, I.; Kokubo, T.; Higashi, H.; Saitoh, S.; Taya, Y.; Yasuda, H.; Ohba, Y.; Nishimura, S.; Tanaka, N.; Okuyama, A. Butyrolactone I, a selective inhibitor of cdk2 and cdc2 kinase. *Oncogene* **1993**, *8*, 2425−2432.

(37) Meijer, L.; Thunissen, A. M. W. H.; White, A.; Garnier, M.; Nikolic, M.; Tsai, L. H.; Walter, J.; Cleverley, K. E.; Salinas, P. C.; Wu, Y. Z.; Biernat, J.; Mandelkow, E. M.; Kim, S.-H.; Pettit, G. R. Inhibition of cyclin-dependent kinases, GSK-3β and casein kinase 1 by hymenialdisine, a marine sponge constituent. *Chem., Biol.* **2000**, *7*, 51−63.

(38) Nugiel, D. A.; Etzkorn, A. M.; Vidwans, A.; Benfield, P. A.; Boisclair, M.; Burton, C. R.; Cox, S.; Czerniak, P. M.; Doleniak, D.; Seitz, S. P. Indenopyrazoles as novel cyclin dependent kinase (CDK) inhibitors. *J. Med. Chem.* **2001**, *44*, 1334−1336.

(39) Zimmermann, J. (Ciba-Geigy). Pharmacologically active pyrimidine derivatives and processes for the preparation thereof. PCT WO 95/09853, 1995.

(40) Barvian, M.; Boschelli, D. H.; Cossrow, J.; Dobrusin, E.; Fattaey, A.; Fritsch, A.; Fry, D.; Harvey, P.; Keller, P.; Garrett, M.; La, F.; Leopold, W.; McNamara, D.; Quin, M.; Trumpp-Kallmeyer, S.; Toogood, P.; Wu, Z.; Zhang, E. Pyrido[2,3-d]pyrimidin-7-one inhibitors of cyclin-dependent kinases. *J. Med. Chem.* **2000**, *43*, 4606−4616.

(41) Clare, P. M.; Poorman, R. A.; Kelley, L. C.; Watenpaugh, K. D.; Bannow, C. A.; Leach, K. L. The cyclin-dependent kinases cdk2 and cdk5 act by a random, anticooperative kinetic mechanism. *J. Biol. Chem.* **2001**, *276*, 48292−48299.

(42) Kent, L. L.; Hullcampbell, N. E.; Lau, T.; Wu, J. C.; Thompson, S. A.; Nori, M. Characterization of novel inhibitors of cyclin-dependent kinases. *Biochem. Biophys. Res. Commun.* **1999**, *260*, 768−774.

(43) Davis, S. T.; Benson, B. G.; Bramson, H. N.; Chapman, D. E.; Dickerson, S. H.; Dold, K. M.; Eberwein, D. J.; Edelstein, M.; Frye, S. V.; Gampe, R. T.; Griffin, R. J.; Harris, P. A.; Hassell, A. M.; Holmes, W. D.; Hunter, R. N.; Knick, V. B.; Lackey, K.; Lovejoy, B.; Luzzio, M. J.; Murray, D.; Parker, P.; Rocque, W. J.; Shewchuk, L.; Veal, J. M.; Walker, D. H.; Kuyper, L. F. Prevention of chemotherapy-induced alopecia in rats by CDK inhibitors. *Science* **2001**, *291*, 134−137.

(44) Bramson, H. N.; Corona, J.; Davis, S. T.; Dickerson, S. H.; Edelstein, M.; Frye, S. V.; Gampe, R. T., Jr.; Harris, P. A.; Hassell, A.; Holmes, W. D.; Hunter, R. N.; Lackey, K. E.; Lovejoy, B.; Luzzio, M. J.; Montana, V.; Rocque, W. J.; Rusnak, D.;

Shewchuk, L.; Veal, J. M.; Walker, D. H.; Kuyper, L. F. Oxindole-Based Inhibitors of Cyclin-Dependent Kinase 2 (CDK2): Design, Synthesis, Enzymatic Activities, and X-ray Crystallographic Analysis. *J. Med. Chem.* **2001**, *44*, 4339−4358.

(45) Fry, D. W.; Harvey, P. H.; Bedford, D.; Fritsch, A.; Keller, P. R.; Wu, Z.; Dobrusin, E.; Leopold, W. R.; Fattaey, A.; Garrett, M. D. Cell cycle and biochemical effects of PD0183812, a potent inhibitor of cyclin-dependent kinase 4. *J. Biol. Chem.* **2001**, *276*, 16617−16623.

(46) Jeong, H. W.; Kim, M. R. R.; Son, K. H.; Han, M. Y.; Ha, J. H.; Garnier, M.; Meijer, L.; Kwon, B. M. Cinnamaldehydes inhibit cyclin-dependent kinase 4/cyclin D1. *Bioorg. Med. Chem. Lett.* **2000**, *10*, 1819−1822.

(47) Shewchuk, L.; Hassell, A.; Wisely, B.; Rocque, W.; Holmes, W.; Veal, J.; Kuyper, L. F. Binding mode of the 4-anilinoquinazoline class of protein kinase inhibitor: X-ray crystallographic studies of 4-anilinoquinazolines bound to cyclin-dependent kinase 2 and p38 kinase. *J. Med. Chem.* **2000**, *43*, 133−138.

(48) Sielecki, T. M.; Johnson, T. L.; Liu, J.; Muckelbauer, J. K.; Grafstrom, R. H.; Cox, S.; Boylan, J.; Burton, C. R.; Chen, H.; Smallwood, A.; Chang, C. H.; Boisclair, M.; Benfield, P. A.; Trainor, G. L.; Seitz, S. P. Quinazolines as cyclin dependent kinase inhibitors. *Bioorg. Med. Chem. Lett.* **2001**, *11*, 1157−1160.

(49) Soni, R.; O'Reilly, T.; Furet, P.; Muller, L.; Stephan, C.; Zumstein-Mecker, S.; Fretz, H.; Fabbro, D.; Chaudhuri, B. Selective in vivo and in vitro effects of a small molecule inhibitor of cyclin-dependent kinase 4. *J. Natl. Cancer Inst.* **2001**, *21*, 436−446.

(50) Lane, M. E.; Yu, B.; Rice, A.; Lipson, K. E.; Liang, C.; Sun, L.; Tang, C.; McMahon, G.; Pestell, R. G.; Wadler, S. A novel cdk2-selective inhibitor, SU9516, induces apoptosis in colon carcinoma cells. *Cancer Res.* **2001**, *61*, 6170−6177.

(51) Carini, D. J.; Kaltenbach, R. F.; Liu, J.; Benfield, P. A.; Boylan, J.; Boisclair, M.; Brizuela, L.; Burton, C. R.; Cox, S.; Grafstrom, R.; Harrison, B. A.; Harrison, K.; Akamike, E.; Markwalder, J. A.; Nakano, Y.; Seitz, S. P.; Sharp, D. M.; Trainor, G. L.; Sielecki, T. M. Identification of selective inhibitors of cyclin dependent kinase 4. *Bioorg. Med. Chem. Lett.* **2001**, *11*, 2209−2211.

(52) Kim, K. S.; Kimball, S. D.; Misra, R. N.; Rawlins, D. B.; Hunt, J. T.; Xiao, H. Y.; Lu, S.; Qian, L.; Han, W. C.; Shan, W.; Mitt, T.; Cai, Z. W.; Poss, M. A.; Zhu, H.; Sack, J. S.; Tokarski, J. S.; Chang, C. Y.; Pavletich, N.; Kamath, A.; Humphreys, W. G.; Marathe, P.; Bursuker, I.; Kellar, K. A.; Roongta, U.; Batorsky, R.; Mulheron, J. G.; Bol, D.; Fairchild, C. R.; Lee, F. Y.; Webster, K. R. Discovery of aminothiazole inhibitors of cyclin-dependent kinase 2: synthesis, X-ray crystallographic analysis, and biological activities. *J. Med. Chem.* **2002**, *45*, 3905−3927.

(53) Toogood, P. L. Cyclin-dependent kinase inhibitors for treating cancer. *Med. Res. Rev.* **2001**, *21*, 487−498.

(54) Gray, N.; Détivaud, L.; Doerig, C.; Meijer, L. ATP-site directed inhibitors of cyclin-dependent kinases. *Curr. Med. Chem.* **1999**, *6*, 859−876.

(55) Fischer, P. M.; Lane, D. P. Inhibitors of cyclin-dependent kinases as anti-cancer therapeutics. *Curr. Med. Chem.* **2000**, *7*, 1213−1245.

(56) Pestell, R.; Mani, S.; Wange, C.; Wu, K.; Francis, R. Cyclin-dependent kinase inhibitors: novel anticancer agents. *Exp. Opin. Investig. Drugs* **2000**, *9*, 1849−1870.

(57) Rosiana, G. R.; Chang, Y. T. Targeting hyperproliferative disorders with cyclin dependent kinase inhibitors. *Exp. Opin. Ther. Patents* **2000**, *10*, 1−16.

(58) Sielecki, T. M.; Boylan, J. F.; Benfield, P. A.; Trainor, G. L. Cyclin-dependent kinase inhibitors: useful targets in cell cycle regulation. *J. Med. Chem.* **2000**, *43*, 1−18.

(59) Kaubisch, A.; Schwartz G. K. Cyclin-dependent kinase and protein kinase C inhibitors: a novel class of antineoplastic agents in clinical development. *Cancer J.* **2000**, *6*, 192−212.

(60) Coghlan, M. P.; Culbert, A. A.; Cross, D. A. E.; Corcoran, S. L.; Yates, J. W.; Pearce, N. J.; Rausch, O. L.; Murphy, G. J.; Carter, P. S.; Cox, L. R.; Mills, D.; Brown, M. J.; Haigh, D.; Ward, R. W.; Smith, D. G.; Murray, K. J.; Reith, A. D.; Holder, J. C. Selective small molecule inhibitors of glycogen synthase kinase-3 modulate glycogen metabolism and gene transcription. *Chem. Biol.* **2000**, *7*, 793−803.

(61) Smith, D. G.; Buffet, M.; Fenwick, A. E.; Haigh, D.; Ife, R. J.; Saunders, M.; Slingsby, B. P.; Stacey, R.; Ward, R. W. 3-Anilino-4-arylmaleimides: potent and selective inhibitors of glycogen synthase kinase-3 (GSK-3). *Bioorg. Med. Chem. Lett.* **2001**, *11*, 635−639.

(62) Ryves, W. J.; Harwood, A. J. Lithium inhibits glycogen synthase kinase-3 by competition for magnesium. *Biochem. Biophys. Res. Commun.* **2001**, *280*, 720−725.

(63) Vierfond, J. M.; Mettey, Y.; Mascrier-Demagny, L.; Miocque, M. Cyclisation par amination intramoléculaire dans la série de la pyrazine. *Tetrahedron Lett.* **1981**, *22*, 1219−1222.

(64) Davis, M. L.; Wakefield, B. J.; Wardell, J. A. Reactions of β-(lithiomethyl)azines with nitriles as a route to pyrrolo-pyridines, -quinolines, -pyrazines, -quinoxalines and -pyrimidines. *Tetrahedron* **1992**, *48*, 939−952.

(65) De Bondt, H. L.; Rosenblatt, J.; Jancarik, J.; Jones, H. D.; Morgan, D. O.; Kim, S. H. Crystal structure of cyclin-dependent kinase 2. *Nature* **1993**, *363*, 595−602.

(66) Schulze-Gahmen, U.; Brandsen, J.; Jones, H. D.; Morgan, D. O.; Meijer, L.; Vesely, J.; Kim S. H. Multiple modes of ligand recognition: crystal structures of cyclin-dependent protein kinase 2 in complex with ATP and two inhibitors, olomoucine and isopentenyladenine. *Proteins: Struct., Funct. Genet.* **1995**, *22*, 378−391.

(67) de Azevedo, W. F.; Mueller-Dieckmann, H.-J.; Schultze-Gahmen, U.; Worland, P. J.; Sausville, E.; Kim, S.-H. Structural basis for specificity and potency of a flavonoid inhibitor of human CDK2, a cell cycle kinase. *Proc. Natl. Acad. Sci. U.S.A.* **1996**, *93*, 2735−2740.

(68) Lawrie, A. M.; Noble, M. E.; Tunnah, P.; Brown, N. R.; Johnson, L. N.; Endicott, J. A. Protein kinase inhibition by staurosporine revealed in details of the molecular interaction with CDK2. *Nat. Struct. Biol.* **1997**, *4*, 796−800.

(69) Russo, A. A.; Jeffrey, P. D.; Pavletich, N. P. Structural basis of cyclin-dependent kinase activation by phosphorylation. *Nat. Struct. Biol.* **1996**, *3*, 696−700.

(70) Meijer, L. Chemical inhibitors of cyclin-dependent kinases. *Trends Cell Biol.* **1996**, *6*, 393−397.

(71) Knockaert, M.; Gray, N.; Damiens, E.; Chang, Y. T.; Grellier, P.; Grant, K.; Fergusson, D.; Mottram, J.; Soete, M.; Dubremetz, J. F.; LeRoch, K.; Doerig, C.; Schultz, P. G.; Meijer, L. Intracellular targets of cyclin-dependent kinase inhibitors: identification by affinity chromatography using immobilised inhibitors. *Chem. Biol.* **2000**, *7*, 411−422.

(72) Knockaert, M.; Viking, K.; Schmitt, S.; Leost, M.; Mottram, J.; Kunick, C.; Meijer, L. Intracellular targets of paullones: identification by affinity chromatography using immobilized inhibitor. *J. Biol. Chem.* **2002**, *277*, 25493−25501.

(73) Diehl, J. A.; Cheng, M.; Roussel, M. F.; Sherr, C. J. Glycogen synthase kinase-3β regulates cyclin D1 proteolysis and subcellular localization. *Genes Dev.* **1998**, *12*, 3499−3511.

(74) Rosenblatt, J.; De, Bondt H.; Jancarik, J.; Morgan, D. O.; Kim, S. H. Purification and crystallization of human cyclin-dependent kinase 2. *J. Mol. Biol.* **1993**, *230*, 1317−1319.

(75) Brown, N. R.; Noble, M. E. M.; Lawrie, A. M.; Morris, M. C.; Tunnah, P.; Divita, G.; Johnson, L. N.; Endicott, J. A. Effects of phosphorylation of threonine 160 on CDK2 structure and activity. *J. Biol. Chem.* **1999**, *274*, 8746−8756.

(76) Leslie, A. G. W. *Joint CCP4 and ESF-EAMCB Newsletter on Protein Crystallography.* **1992**, Vol. 26.

(77) CCP4. The CCP4 (Collaborative Computational Project Number 4) suite: Programs for protein crystallography. *Acta Crystallogr. D* **1994**, *50*, 760−763.

(78) Navaza, J. AMoRe: An automated package for molecular replacement. *Acta Crystallogr.* **1994**, *A50*, 157−163.

(79) Murshudov, G. N.; Vagin, A. A.; Dodson, E. J. Refinement of macromolecular structures by the maximum-likelihood method. *Acta Crystallogr. D* **1997**, *53*, 240−255.

(80) Jones, T. A.; Zou, J. Y.; Cowan, S. W.; Kjeldgaard, M. Improved methods for building protein models in electron density maps and the location of errors in these models. *Acta Crystallogr. A* **1991**, *47*, 110−119.

(81) Lamzin, V. S.; Wilson, K. S. Automated refinement of protein models. *Acta Crystallogr. D* **1993**, *49*, 129−147.

(82) Pleasure, S. J.; Page, C.; Lee, V. M. Y. Pure, post-mitotic polarized human neurons derived from NT2 cells provide a system for expressing exogenous proteins in terminally differentiated neurons. *J. Neurosci.* **1992**, *12*, 1802−1815.

(83) Saillé, C.; Marin, P.; Martinou, J. C.; Nicole, A.; London, J.; Ceballos-Picot, I. Transgenic murine cortical neurons expressing human bcl-2 exhibit increased resistance to amyloid beta-peptide neurotoxicity. *Neuroscience* **1999**, *92*, 1455−1463.

(84) Damiens, E.; Baratte, B.; Marie, D.; Eisenbrand, G.; Meijer, L. Anti-mitotic properties of indirubin-3′-monoxime, a CDK/GSK-3 inhibitor: induction of endoreplication following prophase arrest. *Oncogene* **2001**, *20*, 3786−3797.